MODIFIED EPOXY COATINGS ON MILD STEEL: A STUDY OF TRIBOLOGY AND SURFACE ENERGY

Madhuri Dutta, B. Tech.

Thesis Prepared for the Degree of

MASTER OF SCIENCE

UNIVERSITY OF NORTH TEXAS

August 2009

APPROVED:

Witold Brostow, Major Professor
Jincheng Du, Committee Member
Richard F. Reidy, Committee Member and Interim Chair of the Department of Materials Science and Engineering
Nigel Shepherd, Graduate Advisor of the Department of Materials Science and Engineering
Costas Tsatsoulis, Dean of the College of Engineering
Michael Monticino, Dean of the Robert B. Toulouse School of Graduate Studies

Dutta, Madhuri. Modified epoxy coatings on mild steel: A study of tribology and surface energy. Master of Science (Materials Science and Engineering), August 2009, 71 pp., 11 tables, 44 figures, references, 88 titles.

A commercial epoxy was modified by adding fluorinated poly (aryl ether ketone) and in turn metal micro powders (Ni, Al, Zn, and Ag) and coated on mild steel. Two curing agents were used; triethylenetetramine (curing temperatures: 30 ^{o}C and 70 ^{o}C) and hexamethylenediamine (curing temperature: 80 ^{o}C). Variation in tribological properties (dynamic friction and wear) and surface energies with varying metal powders and curing agents was evaluated. When cured at 30 ^{o}C, friction and wear decreased significantly due to phase separation reaction being favored but increased when cured at 70 ^{o}C and 80 ^{o}C due to cross linking reaction being favored. There was a significant decrease in surface energies with the addition of modifiers.

ACKNOWLEDGMENTS

I would like to deeply express my gratitude to my advisor, Prof. Witold Brostow, for invoking in me the spirit of adventure in regard to research and providing me his guidance and persistent help without which this thesis would not have been possible.

I would like to thank my committee member, Dr. Rick Reidy, for not only his time and suggestions but his help in FTIR – ATR graphs and allowing me to use his equipment. I would also like to thank my committee member, Dr. Jincheng Du, for spending his time in reviewing my thesis.

Thanks to Sridhar, Tea, and Juliana for offering their moral support, invaluable suggestions, and true friendship. I would also like to thank Nelson, Eric, Sundeep, Arun, Antariksh, Wei - Lun, and Ming - Te for helping me with various tests.

I am forever indebted to my parents Subramaniam and Phani Bala; and my sister Lalitha for their care and support in every aspect. I am grateful to Shashank for his endless encouragement when I needed it the most and being there for me in every moment.

TABLE OF CONTENTS

Page

LIST OF TABLES

Page

LIST OF FIGURES

Page

CHAPTER 1

EPOXY COATINGS

1.1 Epoxy

1.1.1 Introduction

Epoxies are an important class of thermosetting polymers that cure (polymerize and crosslink) when mixed with a catalyzing agent or hardener. Epoxies are noted for their versatility, high resistance to chemicals, outstanding adhesion to a variety of substrates, toughness, high electrical resistance, durability at high and low temperatures, low shrinkage upon cure, flexibility, and the ease with which they can be poured or cast without forming bubbles [1 – 5]. These properties make them eligible for use in various applications such as protective coatings (for appliance, automotive primers, pipes) [6, 7], encapsulation of electrical and electronic devices, adhesives, bonding materials for dental uses, replacement of welding and riveting in aircraft and automobiles, composites materials in space industry, printed circuitry, pressure vessels and pipes, and construction uses such as flooring, paving, and airport runway repair [1, 8].

Despite of these advantages, there are also some drawbacks of epoxies which include poor oxidative stability, moisture sensitivity, thermal stability limited to 170°C to 230°C [1, 9], brittle nature owing to their highly cross – linked structures [10], low wear resistance, low scratch resistance and high friction [11].

Properties of uncured epoxy resins such as viscosity which are important in processing as well as final properties of cured epoxies such as strength or electrical

resistance can be optimized by appropriate selection of the epoxy monomer and the curing agent or catalyst [12 – 14].

1.1.2 Chemical Structure

The term 'epoxy' refers to a chemical group consisting of an oxygen atom bonded to two carbon atoms that are already bonded in some way. The simplest epoxy is a three member ring structure known by the term 'α – epoxy' or '1, 2 – epoxy'. The idealized chemical structure is shown in Figure 1 and is the most easily identified characteristic of any other complex epoxy molecule:

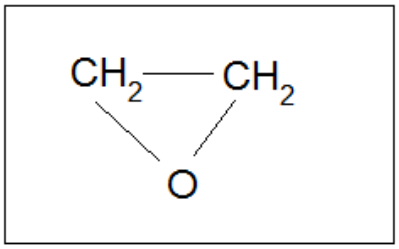

Figure 1. Idealized chemical structure of a simple epoxy (ethylene oxide).

Epoxy resins are formed from a long chain molecular structure with reactive sites (formed by epoxy groups) at either end. The epoxy molecule contains two ring groups at its center which are able to absorb both mechanical and thermal stresses better than linear groups and therefore give the epoxy resin very good stiffness, toughness and heat resistant properties [15] (Figure 2).

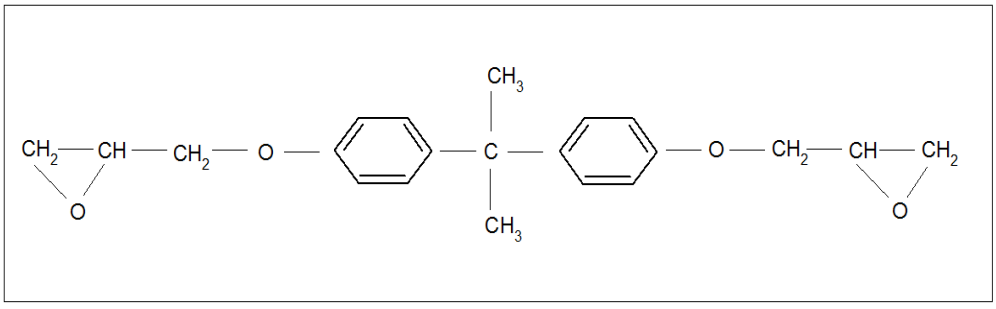

Figure 2. Idealized chemical structure of a typical epoxy.

1.1.3 Diglycidyl Ether of Bisphenol A (DGEBA)

DGEBA resin is the basis for all epoxy resins. Bisphenol A is produced by reacting phenol with acetone under suitable conditions. The “A” stands for acetone, “phenyl” means phenol groups and “bis” means two. Thus, bisphenol A is the product made from chemically combining two phenols with one acetone. Unreacted acetone and phenol are stripped from bisphenol A, which is then reacted with a material called epichlorohydrin. This reaction connects the two (“di”) glycidyl groups on ends of the bisphenol A molecule. The resultant product is the diglycidyl ether of bisphenol A, or the basic epoxy resin. It is these glycidyl groups that react with the amine hydrogen atoms of hardeners to produce the cured epoxy resin [16].

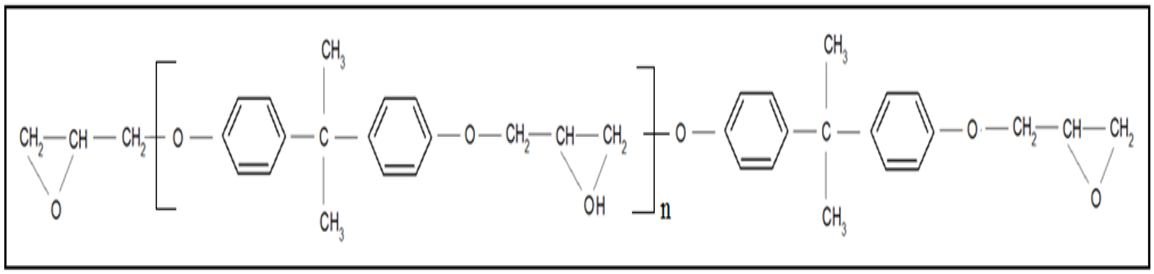

Figure 3. Structure of DGEBA.

1.2 Epoxy Coatings

1.2.1 Introduction

Coatings are widely used in optical, microelectronic, packaging, biomedical and decorative applications. The traditional choice of specific coatings on a cost/performance basis has to a large extent been altered because of safety and health standards, and air pollution [2]. There has been extensive research and development in the area of coatings along certain lines such as water based, continuous solids and powder coatings. A wide variety of modified polymer coatings for specific properties

have been reported in literature. Examples of such coatings include: acrylic coatings with copper nanofillers for harder coatings with a combination of high elastic modulus, scratch resistance and wear resistance [17], hyperbranched nanocomposite coatings for scratch resistance, adhesion and flexibility [18], corrosion resistant polyaniline coatings [19, 20], polystyrene modified with oligostyrenes coatings for adhesive and anti corrosive properties [21], silica/fluoropolymer hydrophobic coatings for rust – resistance, coatings for anti fog and self cleaning applications [22], and self healing coatings [23]. However, since the topic of my research is epoxy coatings, there is focus on epoxy coatings in this thesis.

The first important commercial utilization of epoxy resins for surface coatings in the United States occurred in the late 1940s. Some of these early applications were in floor finishes, maintenance and appliance finishes, overprint varnishes in the metal decorating field, and automotive primers. The esters of the epoxy resins were the binders in these early products; they were derived from the bisphenol A type of resins. A major part of this early work was done by S. Green Lee and his co workers at Devoe and Raynolds Company [24, 25]. Epoxy coatings hold prime position in the coating industry due to their overall good properties: chemical and corrosion resistance, good mechanical properties, excellent adhesion to a variety of substrates, and dielectric properties, high tensile, flexural and compressive strength and thermal stability [26, 27].

There are various ways of coating polymers over metals, some of them are spin coating, dip coating, powder coating or applying the polymer with a brush. Due the nature of my polymer systems, the technique used in my project is application with a brush.

1.2.2 Modified Epoxy Coatings

Modification of epoxies for achieving a wide variety of properties including the above mentioned properties has been very effective. Research in the subject of modification of epoxies (bulk and coating as well) has been active for a long time: Bazyliak, Bratychak, and Brostow proposed the use of oligomers containing peroxy groups as epoxy modifiers in order to improve adhesion [28 – 30]. Fluoropolymer modified epoxy provides better scratch resistance, low surface tension, better overall tribological properties and hydrophobicity [9, 11, 31, 32]. Kumar, Alagar and Mohan developed siliconized epoxy interpenetrating coatings over mild steel wherein Zn powder was used for achieving good corrosion resistance [33]. Saravanan and his group worked on polyaniline pigmented epoxy coatings for protecting steel against corrosion in concrete environments [34]. A different kind work was conducted by Palraj, Selvaraj and Jayakrishnan, where the corrosion and adhesion properties of phosphate coatings on the performance of epoxy primer on galvanized steels was studied [35]. There has also been work reported on blends of thermoplastics like polysulfones and poly(methyl methacrylate) with epoxies for achieving toughness [36, 37]. Studies of multi walled carbon nanotubes added to an epoxy to serve as corrosion protection coating on steels have also been reported [38]. Kumar, Balakrishnan, Alagar and Denchev used silicone and phosphorus for modifying an epoxy to achieve anticorrosion, antifouling and flame retardant properties [39]. Polymers obtained from sustainable resources like *Annona squamosa* oil epoxy had been used by Ahmad and his group as anticorrosive coatings on Fe and Al alloys [40]. Epoxy powder coatings modified using nano – $CaCO_3$, resulting in tensile and corrosion resistant properties were reported by

Yu and his group [41]. Velan and Bilal developed siliconized epoxy with impact and thermal properties for automobile and aerospace applications [42].

1.3 Metallic Particles in Polymers

One of the ways of improving the properties of polymers is by introducing a metallic dispersed phase. Metallic materials have useful properties and characteristics that are crucial for many applications; among them high electric conductivity, paramagnetism, high thermal conductivity as well as good mechanical properties are the most important ones. Combination of polymer + metal results in materials with electrical and magnetic properties comparable with the properties of metals and with a significant improvement in thermal properties. Also, the processability is the same as for the neat polymer, which adds as a great advantage for speed of production and processing costs.

Following is a review of some work reported in the literature on the effects of introducing a metallic or metal oxide phase in a polymer matrix:

Nano ZnO with neoprene rubber was studied by Begum, Yusuff and Joseph; apparently addition of a lower dosage of ZnO was sufficient for improving mechanical properties of the compound [43]. Addition of pure Zn powder to an epoxy phase provides corrosion resistance [33]. Al particles added to poly(ethylene oxide) have affected electric conductivity as studied by Muszynska and her colleagues [44]. They have found that only 1 – 2 wt.% is needed in order to increase the conductivity of the pure polymer. Mamunya et al. used Cu and Ni powders as fillers in an epoxy resin and in poly(vinyl chloride) and studied the concentration dependence of the electric and thermal conductivity [45]. Arshak et al. added a soft Al – Fe – Si magnetic powder to a

polymeric matrix to produce magnetic films to be used for shielding of electromagnetic waves [46].

Metallic particles are added to polymers to improve their mechanical properties as well. Brito and Sanchez [47] used Zn, Cu and Al as fillers in thermoset polymer systems composed by epoxy and amino resins at several concentrations up to 30 wt. %; they studied mechanical properties as well as thermal decomposition. They observed that the temperature of decomposition decreases when metal is added to the epoxy + amino resins, this is true for all metals and all epoxy: amino ratios. Gosh and Maiti prepared polypropylene composites with Ag powder as filler and studied their mechanical properties and observed that there was an improvement in flexural modulus and strength with increase in filler content due to an increase in rigidity [48]. The mechanical properties vary with the type of metal, shape and size of the metallic particles, the type of polymer used and also the process used in the production of such materials and dispersion. Olea – Meija developed a variety of thermoplastic polymer composite systems with micro and nano metal powders of Al, Ni, and Ag and carried out tribological and wear studies along with determination of mechanical properties [49]. Before that uniformity of the powder distribution was verified by a combination of focused ion beam (FIB) + scanning electron microscopy (SEM) technique developed for the purpose [50].

CHAPTER 2

CHARACTERIZATION OF POLYMER COATINGS

This chapter deals with some of the characterization techniques that have been used to study the epoxy coatings created for this project.

2.1 Tribological Tests

The word tribology is derived from the Greek word *tribos* meaning rubbing and *logy* meaning study of, or science. Thus, tribology is defined as “the science and technology of interacting surfaces in relative motion”. The tribological characterization of materials deals with friction coefficient, wear resistance and design of interactive surfaces in relative motion. Friction, wear and lubricant science, are all included in this meaning.

In recent years, friction and wear problems have attracted increased attention in many technically and economically advanced countries of the world. This is mainly due to the fact that about one third of our global energy consumption is consumed wastefully in friction. In 1966, an important landmark in the development of the subject was the publication by Peter Jost and his panel. The report indicated that if the best techniques in machine design and operation were utilized, nearly 500 million British pounds per year could be saved [51 – 53].

Friction and wear in solid bodies are quite complex multi – functional processes, which involve the interaction of their surface layers and which are accompanied by a change in the structure and properties of materials under the influence of load, temperature and the active ingredients in the surrounding medium. The purpose of research in tribology is to understand its mechanisms and eliminate the losses resulting

from friction and wear. Research in tribology leads to greater plant efficiency, better performance, fewer breakdowns, and significant savings in materials and expenses. Although friction is generally considered a nuisance, there are circumstances where on the credit side are important devices such as clutches, brakes, friction and traction devices.

Tribology in polymers is crucial to many applications, since polymeric materials vital in rolling and sliding are now standard in automobiles, machinery, airplanes, computers, etc. Solid lubricants, reinforcing fibers and inorganic particulates have been normally used to enhance those properties [54, 55]. Fillers (whose hardness and modulus are greater than those of the polymer) in the form of particulates and fibers are often embedded into a polymeric matrix to improve its mechanical properties, adhesion properties and aid in creating transfer films by tribochemical reactions [56]. Zhang et al. reported the reduction in wear resistance and friction coefficient when nanosilica and nanoalumina were incorporated into the epoxy matrix [57 – 61]. However, Xu and Mellor studied the effects of fillers on the wear resistance of thermoplastic polymeric coatings and found that silica and dolomite filled polymeric coatings had a higher wear rate than an unfilled polymer [62]. Larson et al. reported that addition of CuO increases wear relative to the neat epoxy [63]. Thus, dispersed fillers seem to be a two – edged sword in modification of tribological properties.

2.1.1. Friction

Friction is the resistance encountered when one body moves tangentially over another with which it is in contact. This resistance force is the friction force. Figure 4 shows the force diagram for a block on ground. Arrows are vectors indicating directions

and magnitudes of forces. W is the force of weight, N is the normal force, F is an applied force of unidentified type, and F_f is the friction force which is equal to the friction of material (μ) times the normal force.

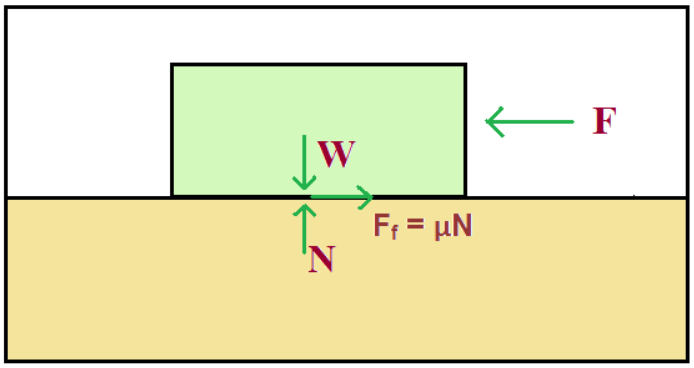

Figure 4. Schematic illustration of a block on ground.

Friction is of two types: static friction and dynamic friction. When two objects slide past each other, a small amount of force will result in no motion. Static friction is the force that is required to initiate motion. If a little more force is applied, the object "breaks free" and slides, although still force needs to be applied for the object to keep sliding. This is kinetic or dynamic friction. The static friction is either higher than or equal to the kinetic friction force.

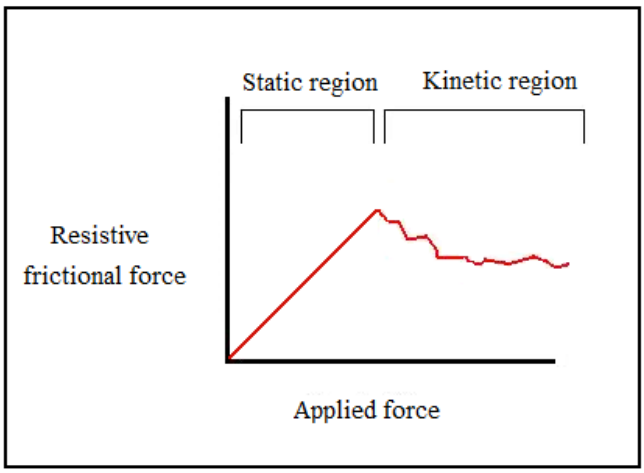

Figure 5. General friction plot.

However, friction is *not* a material property; it is a system property (including environment). Friction mainly depends on operating temperature, roughness of the materials, atmosphere (air, nitrogen, vacuum), presence of a lubricant, and speed of motion. Same materials can show varying friction values with varying system parameters. Therefore, friction results for material pairs that have been tested in different conditions cannot be compared. However, by comparing different material pairs in the same conditions, we can have an idea of how a material pair behaves with respect to other such pairs.

In reality, there are no perfectly flat surfaces; there is always a degree of roughness because of asperities inherent to all surfaces; friction is due to the interaction between these asperities which results in energy dissipation. The contact between the asperities of the materials is responsible for the friction of the system. The real contact area is the sum of the contact area of the asperities and is much smaller than the apparent contact area.

2.1.2 Friction Tests

There are various techniques to determine the friction of materials. The essential feature of any technique for the determination of frictional interaction is a means of applying a known normal load between the two test surfaces which simultaneously carry a measurable tangential force; it must be possible to increase this force until either detectable, or steady relative motion is achieved. The most popular technique is the pin on disc testing, which has been used for my work. However, there are several other techniques like testing using an universal mechanical tester and friction sled according to ASTM D1894 – 08 standard [49, 64], determination of the breakaway friction

characteristics of rolling element bearings according to ASTM G182 – 06 standard, or measuring rolling friction using ASTM G194 – 08 standard. These techniques have not been discussed further in this project.

2.1.2.1 Pin on Disc Tribometry

The pin on disc tester measures the friction and rolling wear properties of dry or lubricated surfaces of a variety of bulk materials and coatings. A pin on disc tribometer operates on the following principle: a flat, pin or sphere is loaded onto the test sample with a precisely known weight. The highly stiff elastic arm insures a nearly fixed contact point and thus a stable position in the friction track. Dynamic friction is determined during the test by measuring the deflection of the elastic arm of by direct measurement of the change in torque. The normal load, rotational speed, and the wear track diameter are all usually controlled parameters. This technique can be used to determine friction not only for polymer based materials but for diamond like carbon coatings, thin films or electronic materials. Most pin on disc testers are computer controlled and store the measured friction versus time or distance plots for future reference. Figure 6 shows a schematic of a pin on disc apparatus.

The test is relatively fast and the normal range of operational parameters are covered within 2 h. Another advantage of the test is the possibility to measure the local friction effect, which is of interest when relating measurements to simulations. Also, influential parameters such as temperature, environmental gasses (air, nitrogen, oxygen, etc) can be controlled.

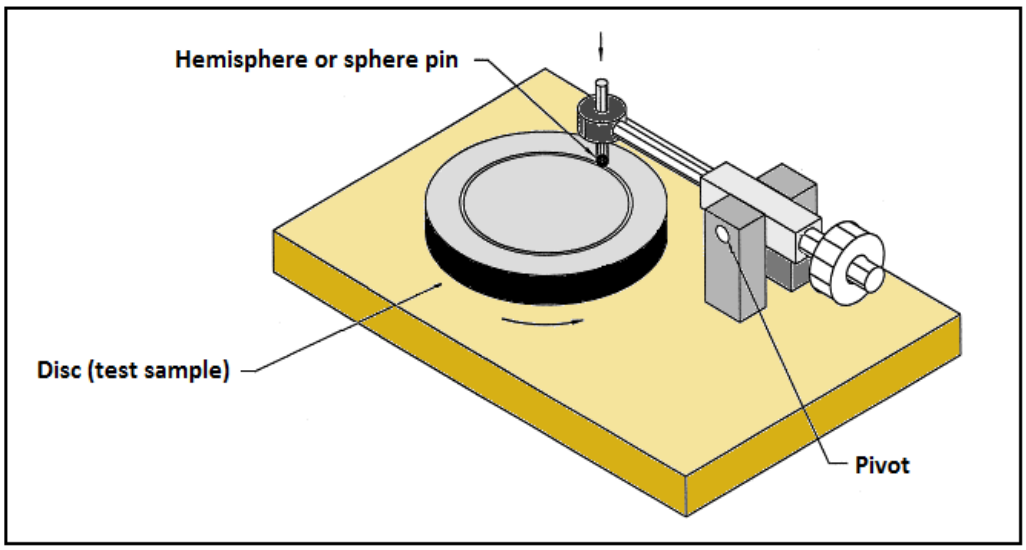

Figure 6. Schematic of the pin on disc test.

2.1.3 Wear

Wear is the progressive damage, involving material loss, which occurs on the surface of a component as a result of its motion relative to the adjacent working parts; it is an almost inevitable companion of friction. The economic consequences of wear are widespread and pervasive; they involve not only the costs of replacement parts, but also the expenses involved in machine downtime, and lost production. A further significant factor can be the decreased efficiency of worn plant and equipment which can lead to both inferior performance and increased energy consumption. Wear rate of a rolling or sliding contact is conventionally defined as the volume lost from the wearing surface per unit sliding distance. The wear rate depends on various parameters: operating temperature, normal load, relative sliding speed, amount of lubrication, thermal, mechanical, and chemical properties of the materials in contact. If the interface is contaminated by solids third bodies (like dirt) the situation can be more complex.

Similar to friction, wear is not a material property but depends on the above mentioned parameters. Usually materials exhibiting high friction also exhibit high wear

rate. However, this is not true always. Materials like polymers or interfaces with solid lubricants exhibit low friction but relatively high wear rates.

2.1.4 Wear Tests

Early research on wear was started by Bely [65] and is continued by Mishkyn, Petrokovets and coworkers in Homel, Belarus [66, 67, 68]. Wear is of different types:

- Melt wear: Sometimes localized melting of the uppermost layer of the wearing solid may occur.
- Oxidational wear: It results due to the oxidation of the wearing material. The oxides are formed either under dry sliding or lubricated conditions by either rubbing metal against metal or metal against ceramic. These oxides reduce wear and friction of metals by preventing severe metal to metal contact. Atmospheres and lubricants play a very important role in the oxidational wear mechanism [69].
- *Adhesive wear:* Adhesive wear occurs because of shearing points of contact or asperities that undergo adhesion or cold welding. For adhesive wear to occur it is necessary for the surfaces to be in intimate contact with each other. Surfaces which are held apart by lubricating films, oxide films etc. reduce the tendency for adhesion to occur.
- *Abrasive wear:* Abrasive wear is damage to a component's surface which arises because of the motion relative to that surface of either harder asperities or perhaps hard particles trapped at the interface. It could also arise if the counterface is both rough and intrinsically harder than the wearing component.

– *Fatigue wear*: Fatigue is known to be a change in the material state due to repeated (cyclic) stressing which results in progressive fracture. Microscopic wear caused by fatigue may be accompanied by “pitting” – macroscopic crumbling out caused by fatigue in individual surface sections of polymer based materials [65].

Wear can be determined using various techniques. The technique used for my project is determining the volume loss by measuring the wear track resulted due to the pin on disc friction test as suggested by the G99 – 05 standard. Wear is calculated by measuring the dimensions of the groove produced by the pin after the pin on disc test. This can be done using a Scanning Electron Microscope (SEM) or a profilometer. However, wear can also be calculated by mass loss measurement as described by the G99 – 05 standard. The results are reported as volume loss or wear rate of the sample in cubic millimeters or wear rate of the sample in during sliding. Sliding wear can also be calculated by scratch testing as well [32, 70 – 72].

2.1.5 Surface Properties

2.1.5.1 Contact Angle

Consider a liquid droplet resting on a flat, solid surface. The angle formed between the two interfaces at the three – phase line contact is known as the contact angle. The contact angle determines whether the liquid wets the solid or not. If the liquid is very strongly attracted to the solid surface (i.e., in the case of water the solid is strongly hydrophilic) the droplet will completely spread out on the solid surface and the contact angle will be close to 0°. Less strongly hydrophilic solids will have a contact angle up to 90°. If the surface is highly hydrophilic, contact angles will be between 0° to

30°. If the solid surface is hydrophobic and the liquid, like water the contact angle will be larger than 90°. On highly hydrophobic surfaces, the water contact angles are as high as 150° or even nearly 180°. On these surfaces, water droplets simply rest on the surface, without actually wetting to any significant extent (examples of such kind are fluorinated surfaces like Teflon). A schematic of this explanation in shown in Figure 7. Liu, Chen and Xin developed super hydrophobic surfaces using silica/fluoropolymer inspired by the behavior of lotus leaves which exhibit a self cleaning effect [73].

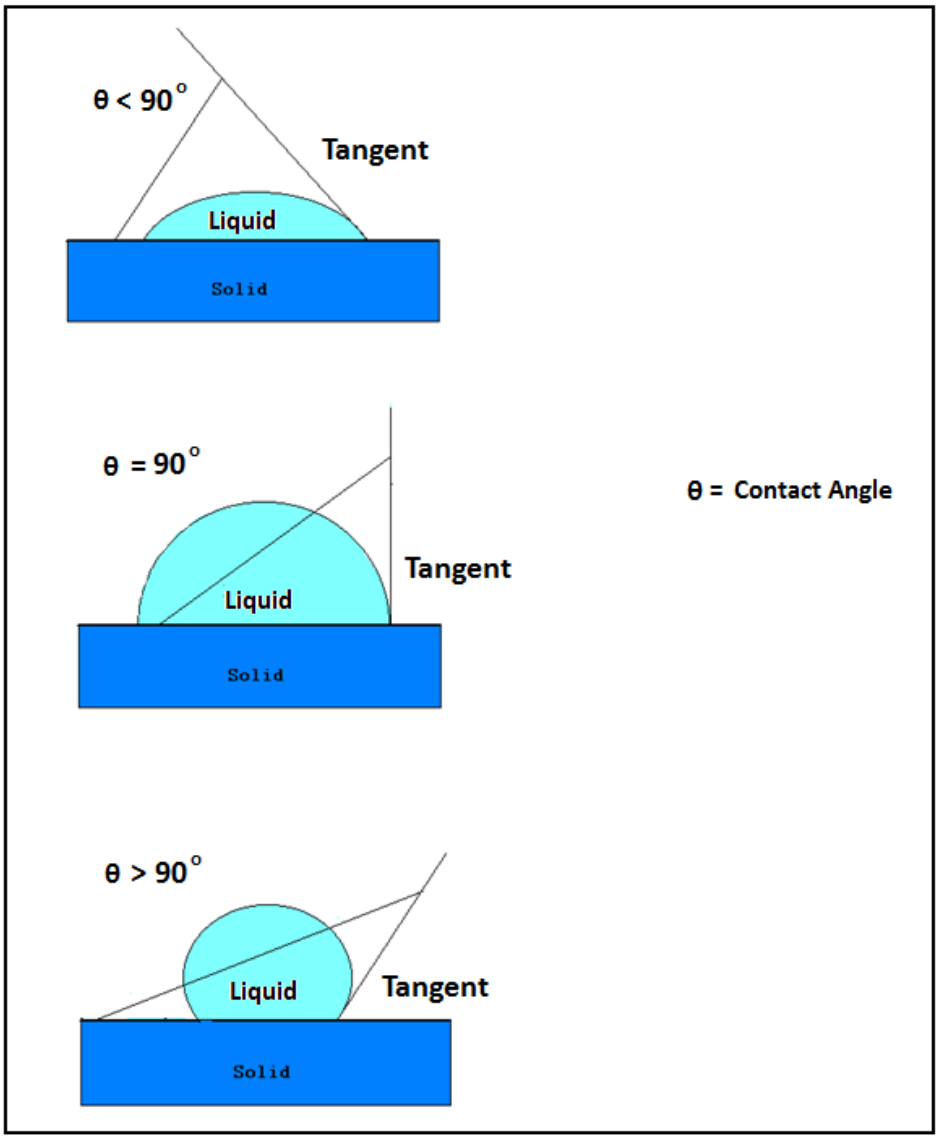

Figure 7. Schematic of the contact angle forms by a liquid droplet.

In general, two different approaches are commonly used to measure contact angles of non – porous solids: goniometry and tensiometry. Goniometry involves the observation of a sessile drop of test liquid on a solid substrate. Tensiometry involves measuring the forces of interaction as a solid is contacted with a test liquid. The technique used for my project is sessile drop goniometric technique. The practical applications of determining the contact angle include: surface cleanliness determination, wettability, adhesion, and surface treatment and coatings evaluation.

2.1.5.2 Surface Energy

Wetting ability of a liquid is a function of the surface energies of the solid – gas interface, the liquid – gas interface and the solid – liquid interface. The surface energy across an interface or the surface tension at the interface is a measure of the energy required to form a unit area of new surface at the interface. The intermolecular bonds or cohesive forces between the molecules of a liquid cause surface tension. When the liquid encounters another substance, there is usually an attraction between the two materials. The adhesive forces between the liquid and the second substance will compete against the cohesive forces of the liquid. Liquids with weak cohesive bonds and a strong attraction to another material (or the desire to create adhesive bonds) will tend to spread over the material. Liquids with strong cohesive bonds and weaker adhesive forces will tend to form a droplet when in contact with another material.

Surface energy measurements can be carried out using dyne pen method, contact meter method or tensiometer. However, the first two methods can be used on substrates or on dry coatings but the tensiometer method is restricted to solids where all exposed faces have the same composition.

Surface energy can be related to the contact angles by the Young's equation:

$$\gamma_{sg} = \gamma_{sl} + \gamma_{lg} \cos\theta \quad (2.1)$$

where, γ_{sg} = solid – gas interfacial energy,

γ_{sl} = solid – liquid interfacial energy,

γ_{lg} = liquid – gas energy, and

θ = contact angle between the solid and the liquid

2.1.6 Surface Chemistry

The surface chemistry of the coatings can be analyzed by various techniques: X – ray diffraction (XRD), photoelectron spectroscopy (XPS), auger electron spectroscopy (AES), ion scattering spectrometry (ISS), sputtered neutral mass spectrometry (SNMS) and Fourier transform infrared spectroscopy (FTIR).

In this project FTIR with attenuated total reflection (ATR) accessory was used for analyzing the phases present on the surface. In attenuated total reflection infrared (ATR – IR) spectroscopy, the infrared radiation is passed through an infrared transmitting crystal with a high refractive index at such an angle that it is totally internally reflected at each reflection it makes inside the crystal. The solid sampling surface is pressed into intimate optical contact with the top surface of the crystal such as Si, ZnSe or Ge. At each reflection a part of the light, called the evanescent wave passes beyond the crystal interface and interacts with the sample in contact with the crystal. At the output end of the crystal, the beam is directed out of the crystal is collected by a detector.

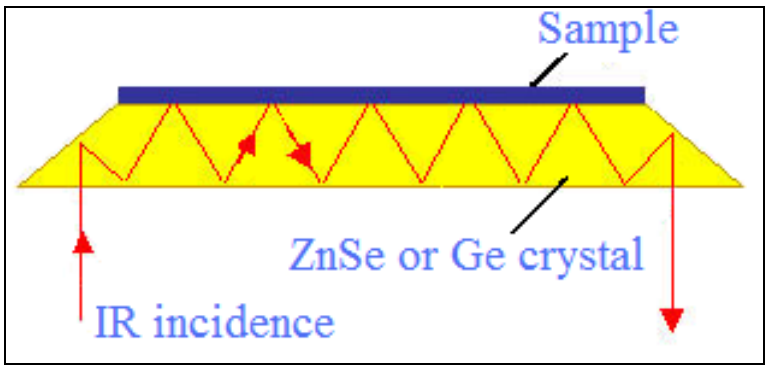

Figure 8. Schematic of ATR experiment.

2.1.7 Surface Roughness

Surface roughness most commonly refers to the variation in the height of the surface relative to a reference plane. To measure surface profile, in order to quantify its roughness, the most widely used techniques are profilometery or atomic force microscopy (AFM). Profilometery has been used in this project for its ease of testing.

Profilometers are of two types: contact profilometers and non – contact profilometers. In a contact profilometer, a diamond stylus is moved vertically in contact with a sample and then moved laterally across the sample for a specified distance and specified contact force. Small surface variations in vertical stylus displacement can be measured as a function of position. The height position of the diamond stylus generates an analog signal which is converted into a digital signal stored, analyzed and displayed. Whereas an optical profilometer is a non – contact method for providing much of the same information as a stylus based profilometer.

2.1.8 Metal Powder Analysis

XRD and SEM are among the various techniques available for the analysis of metal powders in terms of morphology and particle size.

X – ray powder diffraction analysis is a powerful method by which X – rays of a known wavelength are passed through a sample to be identified in order to identify the crystal structure. Due to their wave nature, X – rays are diffracted by the lattice of the crystal to give a unique pattern of peaks of 'reflections' at differing angles and of different intensity. The diffracted beams from atoms in successive planes cancel unless they are in phase, and the condition for this is given by the Bragg's relationship:

$$n\lambda = 2d\ sin\theta \tag{2.2}$$

where, n = Integer determined by the order given

λ = Wavelength of the X – rays

d = Distance between different plane of atoms in the crystal lattice

θ = Angle of diffraction

The X – ray detector moves around the sample and measures the intensity and position (2θ) of these peaks. This data is plotted as intensity vs. position angle to give a series of "peaks" or "lines", which is called the diffraction pattern. Each chemical compound or phase reflects X – rays slightly differently and so has a different diffraction pattern. A mixture of compounds gives a pattern that is made up of the patterns of all the individual compounds. So to identify the compounds present in a mixture the pattern obtained is compared to a large database of patterns. XRD analysis can also be used for investigating the structure of crystalline materials, from atomic arrangement to crystallite size and imperfections, texture or even stress analysis of polycrystalline materials (like powders).

SEM uses a focused beam of high – energy electrons to generate a variety of signals at the surface of solid specimens. The signals that derive from electron –

sample interactions reveal information about the sample including external morphology (texture), chemical composition, and crystalline structure and orientation of materials making up the sample.

2.1.9 Other tests

There are several other tests for characterizing polymer coatings: scratch test, adhesion test, tensile test, etc. However, for the sake of this project these tests have not been covered.

CHAPTER 3

MATERIALS AND EXPERIMENTAL PROCEDURE

3.1 Materials

3.1.1 Epoxy

Epon™ Resin 828, an undiluted clear difunctional bisphenol A / epichlorohydrin derived liquid epoxy resin (diglycidyl ether of bisphenol A) was used as the base epoxy in this project. This epoxy resin as discussed in Chapter 1 is the basis for all epoxy resins. The resin was obtained from Hexion Speciality Chemical Inc. The T_g of the epoxy is 92 ^oC [31].The chemical structure of the resin is shown in Figure 3. The typical properties of the resin are shown below:

Property	Value
Glass transition temperature (T_g) °C	92
Epoxide equivalent weight g/eq	185 - 192
Viscosity @ 25 °C P	110 - 150
Density @ 25 °C g/ml	1.16

Table 1. Typical properties of EPON™ Resin 828 [74].

3.1.2 Modifiers

3.1.2.1 Fluoropolymer

Fluorinated poly(aryl ether ketone) (12 FPEK) fluoropolymer was used as one of the modifiers. The main aim of using 12 FPEK was due to its low surface energy nature which could provide hydrophobicity to the material and for its scratch resistance [32].

The 12 FPEK was synthesized in the Department of Chemistry, Texas State University, San Marcos. The procedure used for synthesizing the fluoropolymer was according to a procedure reported in [75, 76].

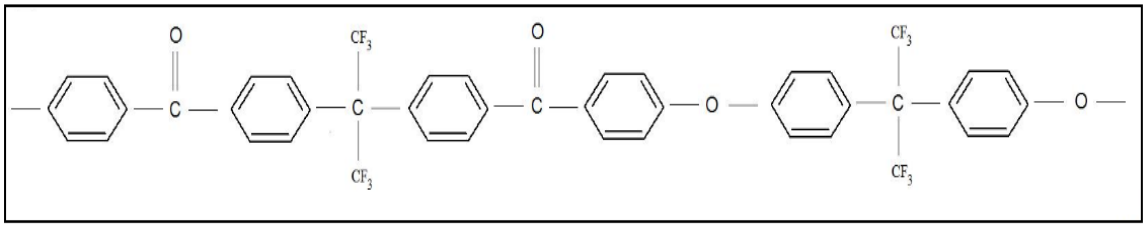

Figure 9. Chemical structure of 12 FPEK [76].

Property	Value
Glass transition temperature (T_g) ^oC	180
Dielectric constant @ 10 GHz	2.4
Soluble in common organic solvents	Yes

Table 2. Properties of 12 FPEK [75].

3.1.2.2 Metallic Fillers

Four types of metal powders of size 1 – 5 μm were used in this project: Ni, Al, Ag, and Zn. Ni for its corrosion resistance, tribological and mechanical properties; Al for low density (when compared to other three metal powders); Ag for high thermal and electrical conductivity and lastly Zn for high corrosion resistance. These metals powders were obtained from Atlantic Equipment Engineers (a division of Micron Metals Inc.). The Ni particles were used in flakes form whereas the Al particles were atomized particles. The shape of Ag was irregular, whereas the Zn particles were as a combination of

irregular and spherical particles. The properties of all the four metal powders are specified in Table 3.

Property	Value			
	Ni	*Al*	*Ag*	*Zn*
Melting Point ^{o}C	1453	660.1	960.8	419
Boiling Point ^{o}C	2730	2467	2210	907
Density g/cm^{3}	8.9	2.699	10.49	7.13
Brinell Hardness MPa @ 20^{o}C	700	245	24.5	412
Electrical Resistivity μΩ-cm	6.84	2.655	1.084	5.92
Crystal Structure	FCC	FCC	FCC	Hex

Table 3. Properties of Ni, Al, Ag and Zn powders [77].

3.1.3 Curing Agents

Two types of curing agents were used in this work. One of them is triethylenetetramine (TETA) – a room temperature curing agent (from Hexion Speciality Chemical Inc.) and the other is hexamethylenediamine (HMDA) – a high temperature curing agent (from Sigma Aldrich). The reason for using two different types of curing agents was to analyze the change in properties with variation in curing temperature. It has been reported in literature that curing temperature has a significant effect over the properties (especially mechanical properties, friction, tensile bond strength, electrical resistivity, etc.) of cured epoxy [78, 79, 31]. The properties of both the curing agents have been given in Figure 13.

Property	Value	
	Triethylenetetramine	Hexamethylenediamine
Amine equivalent mg/g	1,410 – 1,460	-
Density @ 20 °C g/ml	0.98	0.89
Melting Point °C	12	42
Boiling Point °C	227	111 - 130
Flash Point °C	275	94
Molecular Weight g/mol	146.23	116.2

Table 4. Properties of the curing agents.

3.2 Epoxy Modification and Curing

The amount of each component used for the epoxy modification and curing was:

Amount of 12 FPEK: 10 wt.% of the total system

Amount of curing agent:

TETA: 100 g epoxy → 13 g TETA curing agent

HMDA: 100 g epoxy → 15 g HMDA curing agent

Amount of metal powder: 100 g epoxy → 25 wt.% metal powder

Calculated amount of 12 FPEK was dissolved in chloroform (20 ml chloroform / 1 g 12 FPEK) and then the epoxy resin was added. Then calculated amounts of metal powders were in turn added. This mixture was subjected to vacuum at 65 ^{o}C for three hours to remove chloroform and any trapped air. The mixture was manually stirred for 30 min and the curing agents were added accordingly. These epoxy mixtures were coated on to ASTM A366 steel substrates (1” X 2”) using a brush. The composition of

the ASTM A366 steel is specified in Table 5. Before the coating application the steel substrates were degreased using acetone. The systems cured using TETA were cured at two different temperatures: 30 ^{o}C and 70 ^{o}C [31], and the systems cured using HMDA were cured at 80 ^{o}C [33]. Thus, three different types of systems were synthesized using TETA and HMDA. Each system consisted of six compositions:

1. Unmodified epoxy
2. Epoxy + 12 FPEK
3. Epoxy + 12 FPEK + Ni
4. Epoxy + 12 FPEK + Al
5. Epoxy + 12 FPEK + Ag
6. Epoxy + 12 FPEK + Zn

The following curing cycles were employed depending on the curing agent used:

TETA:

Set 1: Cured at 70 ^{o}C (3 h)

Set 2: Cured at 30 ^{o}C (7 days)

HMDA: Cured at 30 ^{o}C (5 h) and then post cured at 80 ^{o}C (24 h)

After curing all the samples were stored at 30 ^{o}C.

Element	**Amount**
Carbon	0.15
Manganese	0.6
Phosphorus	0.03
Sulfur	0.0035

Table 5. Composition of ASTM A366 steel [80].

3.3 Characterization

3.3.1 Friction Determination

Nanovea pin on disc tribometer from Micro Photonics Inc., was used for determining dynamic friction. SS 302 grade stainless steel ball with diameter 3.20 mm was used as the pin. Three values of friction were measured in each case and the mean was calculated. The experimental conditions were:

Radius of wear track: 2.0 mm

Rotation speed: 100.0 rpm

Load: 5.0 N

Revolutions: 500.0, 5000.0

Room temperature

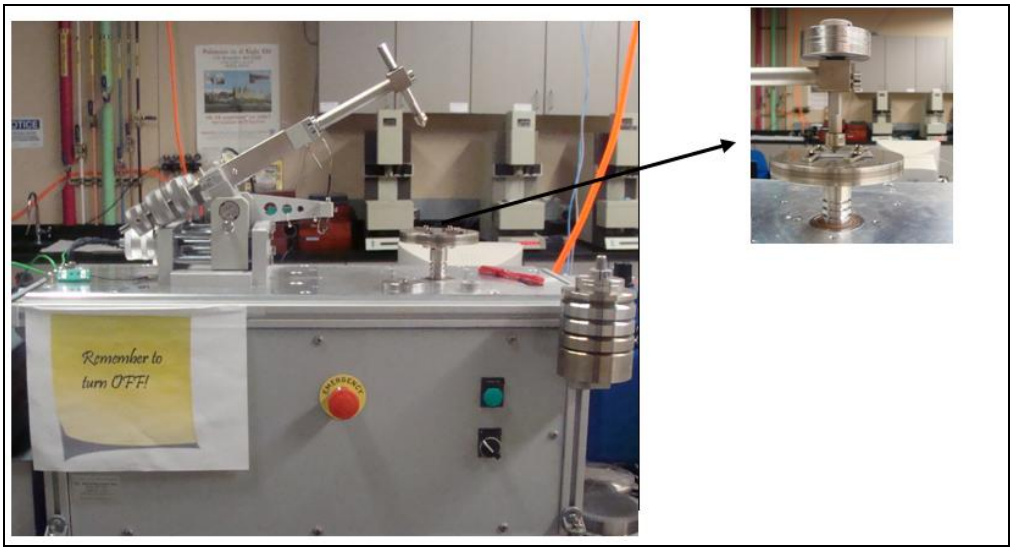

Figure 10. Image of Nanovea pin on disc tribometer.

3.3.2 Wear Determination

Wear was determined by studying the wear track resulted due to the pin on disc friction test after 5000 revolutions. FEI Quanta 200 SEM was used for determining the wear track width. The accelerating voltage was 20.0 kV. Ten values of wear track width

were measured at different locations on each sample and averaged for the purpose of accuracy. Once the wear track width was obtained, the volume loss due to wear was calculated using the following formula as suggested by the ASTM G99 – 05:

$$V_m = 2\pi R \left[r^2 \sin^{-1}\left(\frac{d}{2r}\right) - \left(\frac{d}{4}\right)(4r^2 - d^2)^{\frac{1}{2}} \right] \quad (3.1)$$

where, V_m = disc (test sample) volume loss in mm^3

R = wear track radius in mm *(2.0 mm in this case)*

d = wear track width in mm

r = pin end radius in mm *(1.6 mm in this case)*

Wear rate was then calculated using:

$$K = \frac{V_m}{WX} \quad (3.2)$$

where, K = Wear rate in mm^3 / Nm

V_m = Volume loss due to wear in mm^3

W = Load in N

X = Sliding distance in m

Figure 11. Image of FEI Quanta SEM.

3.3.3 Contact Angle Determination

Sessile drop technique was used for determining contact angles of the coatings to characterize their surface wettability. A Ramé – Hart Instrument co., goniometer was used for this purpose. A polar liquid (water) and an apolar liquid (diiodomethane) were used as testing liquids [81]. Surface tension @ 20 ^{o}C of water and diiodomethane is 72.80 mN/m and 50.80 mN/m respectively [82]. Equal amounts of test liquids were used for the test. Due the nature of the liquids, the amount test drops for water and diiodomethane could not be maintained the same; however, constant amounts were maintained for all tests in each category of tests by rotating 4 divisions on the syringe for testing with water and 1 division for testing with diiodomethane. The mean of five contact angles for each sample was calculated.

Figure 12. Image of Ramé – Hart goniometer.

3.3.4 Surface Energy Determination

The Ramé – Hart goniometer which was used for calculating contact angles was used for determining surface energies of the coatings as well. The surface energy

values are calculated directly by the software using the contact angles obtained in section 3.3.3. Wu's equations (harmonic – method) are used by the software for the surface energy calculations are [83]:

$$(1+\cos\theta_1)\gamma_1 = 4\left(\frac{\gamma_1^d\,\gamma_s^d}{\gamma_1^d+\gamma_s^d}+\frac{\gamma_1^p\,\gamma_s^p}{\gamma_1^p+\gamma_s^p}\right) \tag{3.3}$$

$$(1+\cos\theta_2)\gamma_2 = 4\left(\frac{\gamma_2^d\,\gamma_s^d}{\gamma_2^d+\gamma_s^d}+\frac{\gamma_2^p\,\gamma_s^p}{\gamma_2^p+\gamma_s^p}\right) \tag{3.4}$$

where, θ_1 = Contact angle made by liquid 1 on the solid

θ_2 = Contact angle made by liquid 2 on the solid

γ_1 = Surface tension of liquid 1

γ_2 = Surface tension of liquid 2

γ_1^d = Dispersion component of surface tension of liquid 1

γ_2^d = Dispersion component of surface tension of liquid 2

γ_s^d = Dispersion component of surface energy of solid

γ_1^p = Polar component of surface tension of liquid 1

γ_2^p = Polar component of surface tension of liquid 2

γ_s^p = Polar component of surface energy of solid

All the variables in the above equations are known except for the dispersion and polar components of the surface energy of the solid. The software solves the above mentioned two equations and gives the values for surface energy of the solid.

These equations are according to harmonic – mean method. However, geometric – mean method can also be used but harmonic – mean method is considered accurate

for low energy materials like polymers [83]. Wu's equations to calculate surface energy by geometric – mean method are:

$$(1+\cos\theta_1)\gamma_1 = 2\left((\gamma_1^d\,\gamma_s^d)^{1/2} + (\gamma_1^p\,\gamma_s^p)^{1/2}\right) \quad (3.4)$$

$$(1+\cos\theta_2)\gamma_2 = 2\left((\gamma_2^d\,\gamma_s^d)^{1/2} + (\gamma_2^p\,\gamma_s^p)^{1/2}\right) \quad (3.5)$$

where, θ_1 = Contact angle made by liquid 1 on the solid

θ_2 = Contact angle made by liquid 2 on the solid

γ_1 = Surface tension of liquid 1

γ_2 = Surface tension of liquid 2

γ_1^d = Dispersion component of surface tension of liquid 1

γ_2^d = Dispersion component of surface tension of liquid 2

γ_s^d = Dispersion component of surface energy of solid

γ_1^p = Polar component of surface tension of liquid 1

γ_2^p = Polar component of surface tension of liquid 2

γ_s^p = Polar component of surface energy of solid

3.3.5 Thickness Determination

The thickness of the coatings was measured by cutting each sample into two halves (perpendicular to its length) using a TechCut 4 low speed saw from Allied High Tech. Productions Inc. The speed used for cutting was 250 rpm. The cross section of each sample was analyzed using a Nikon Eclipse ME 60 optical microscope. The thickness of the coatings was calculated by taking the mean of ten thickness values on each sample.

Figure 13. Image of TechCut 4 low speed saw.

Figure 14. Image of Nikon Eclipse ME 60 optical microscope.

3.3.6 Surface Analysis of Coating

The surface composition of the coatings was determined using a Nicolet 6700 Spectrometer with Smart Horizontal ATR micro – sampling accessory from Thermo Electron with 4 cm^{-1} resolution. ATR spectra were collected in the range 800 – 4000 cm^{-1}. The area of the sample to be measured was selected visually and the spring – loaded ATR element was lowered to make contact with the surface of the sample.

Figure 15. Image of Nicolet 6700 Spectrometer.

3.3.7 Surface Roughness

Surface roughness of the coatings was calculated using a Veeco Dektak 150 Profilometer. The profilometer amplifies and records the vertical motions of a stylus displaced at a constant speed by the surface to be measured. As the stylus moves, the stylus rides over the sample surface detecting surface deviations. A stylus with tip radius of 12.5 µm was used. The force applied to the sample was 1 mg, and scan rate was 26.7 µm/s. The scan length was 800 µm and the measurement range was 65.5 µm. The surface roughness can be quantified using average roughness parameters. These parameters usually refer to variations in the height of surface relative to a reference plane. Surface roughness is usually characterized by the center-line average (R_a) and the root mean square average (R_q), skewness (Sk) and kurtosis (K).

Let us consider a profile, z(x) in which profile heights are measured from a reference line. A center line or mean line is defined as the line such that the area between profile and the mean line above the line is equal to that below the mean line. Let L be the sampling length of the profile (profile length). R_a is the arithmetic mean of the absolute values of vertical deviation from the mean line through the profile. R_q is the

root mean square of the arithmetic mean of the square of the vertical deviation from the reference line.

In mathematical form, they can be written as [52]:

$$R_a = \frac{1}{L}\int_0^L \left| z - m \right| dx \tag{3.6}$$

$$m = \frac{1}{L}\int_0^L z\ dx \tag{3.7}$$

$$R_q = \sqrt{\frac{1}{L}\int_0^L (z^2)\, dx} \tag{3.8}$$

The skewness and kurtosis in the normalized form are given as [52]:

$$Sk = \frac{1}{\sigma^3 L}\int_0^L (z-m)^3\ dx \tag{3.9}$$

$$k = \frac{1}{\sigma^4 L}\int_0^L (z-m)^4\ dx \tag{3.10}$$

In this study, only R_a and R_q were determined by scanning line profiles with the profilometer.

Figure 16. Image of Veeco Dektak 150 Profilometer.

3.3.8 Metal Powder Analysis

3.3.8.1 Composition

The metal powders were analyzed for their composition using a Rigaku Ultima III High – Resolution XRD. Cu K – α radiation of wavelength 1.54 A^o was used. Additional acquisition parameters were: 2θ range = 20^o – 90^o and scan rate = 2^o min^{-1}. Diffraction patterns were referenced against the JCPDS database for sample identification.

Figure 17. Image of Rigaku Ultima III high – resolution XRD.

3.3.8.2 Size and Morphology

A pinch of each metal powder was mixed with 20 ml of ethanol was mixed in a sonicator for 30 min. Then 2 drops of each liquid was put onto Al stubs, allowed to dry and studied using an FEI Quanta 200 SEM for its size and morphology. The accelerating voltage was 20.00 kV.

CHAPTER 4

RESULTS AND DISCUSSIONS

4.1 Metal Powder Characterization

4.1.1 Composition

In order to determine the existence of any secondary phases in the metal powders (as they were used in their pure form) XRD was carried out for all the four metal powders (Ni, Al, Ag and Zn). Since the entire work was done in lab atmosphere there was a chance of forming a new secondary phase like a metal oxide phase which would affect the tribological properties of the end coating. Hence, it was pertinent to analyze the composition of the metal powder to determine the existing phases.

Diffraction patterns of Ni, Al and Ag powders didn't show traces of any secondary phases but the diffraction pattern of Zn powder showed some peaks related to ZnO phase (Figures 18 – 21).

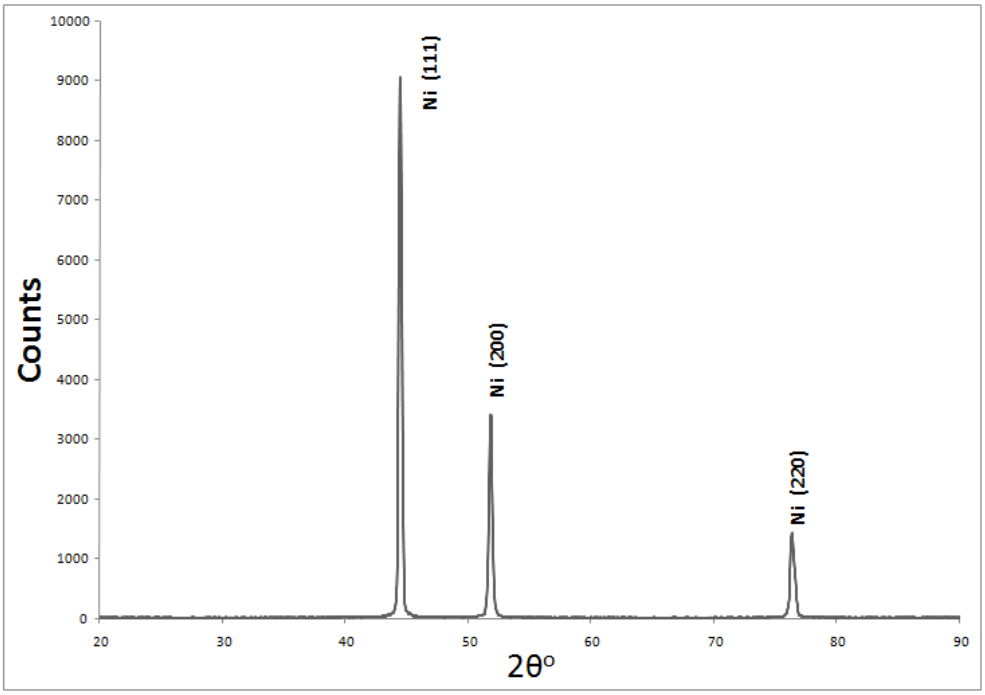

Figure 18. Diffraction pattern of Ni powder.

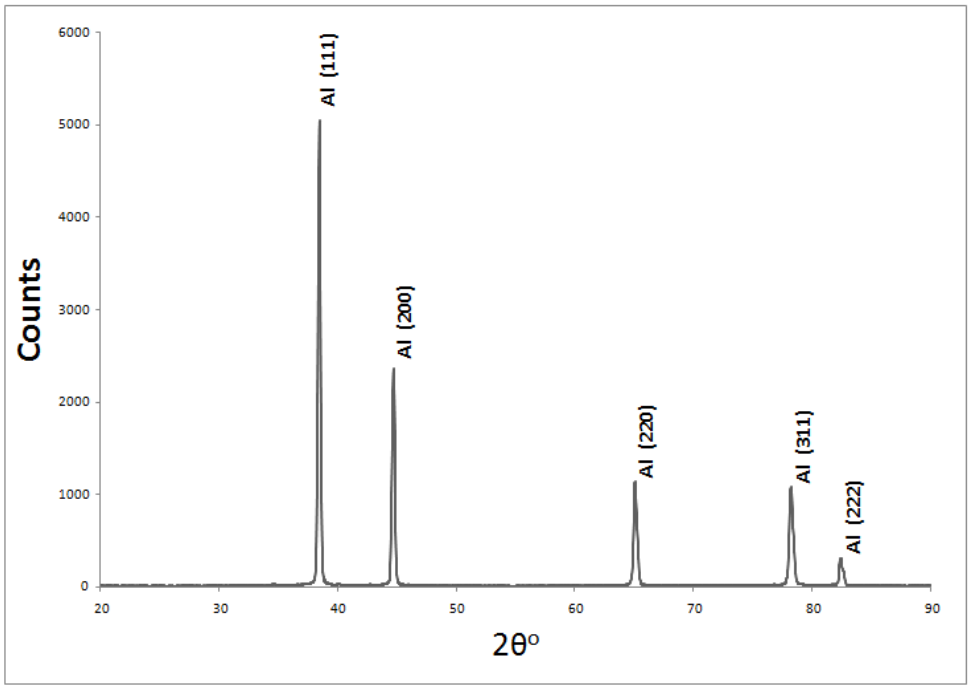

Figure 19. Diffraction pattern of Al powder.

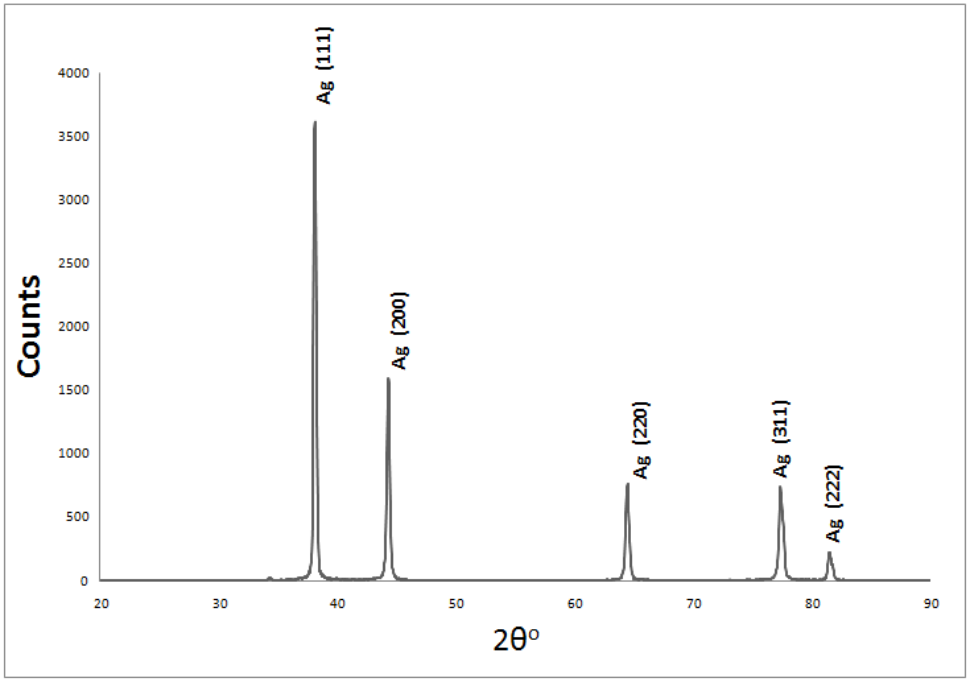

Figure 20. Diffraction pattern of Ag powder.

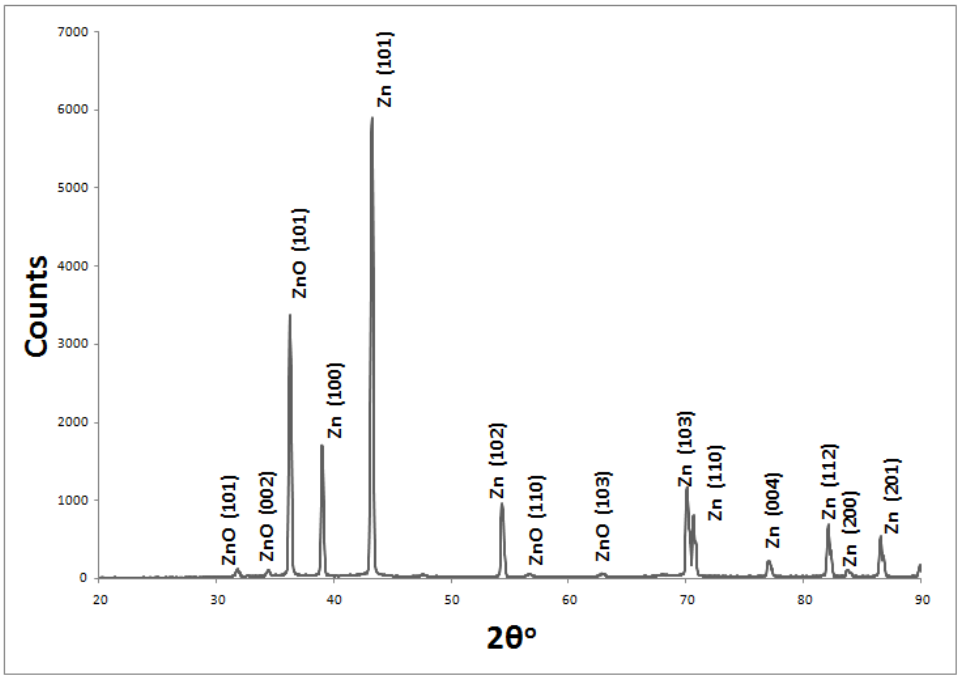

Figure 21. Diffraction pattern of Zn powder.

4.1.2 Morphology

Morphology of the metal particles plays an important role over the properties of the end material. Hence the morphology of the metal powders was studied using an SEM and the average particle size of the powders was calculated using the Image J software. The digital images studied are in high resolution tiff format (1024 x 1024 pixels). The software allows assigning a value of length to each pixel by relating the amount of pixels contained in the micrometric bar of each image. Once the scale is set, measurement of each particle in pixels can be performed, which is directly converted into length units.

Ni particles were used in the flake form (data from Atlantic Equipment Engineers), so the SEM image of Ni particles (Figures 22 a, b) shows particles sharp corners and non – uniform morphology. Al particles were atomized particles (data from Atlantic Equipment Engineers), hence the SEM of Al particles (Figures 23 a, b) shows

spherical particles. Whereas the SEM images of Ag and Zn powders (Figures 24 a, b and 25 a, b) show irregular particles and a combination of spherical and irregular particles respectively.

The calculated average size of the metal powders was:

Ni – 2.5 µm

Al – 2.6 µm

Ag – 3.2 µm

Zn – 2.6 µm

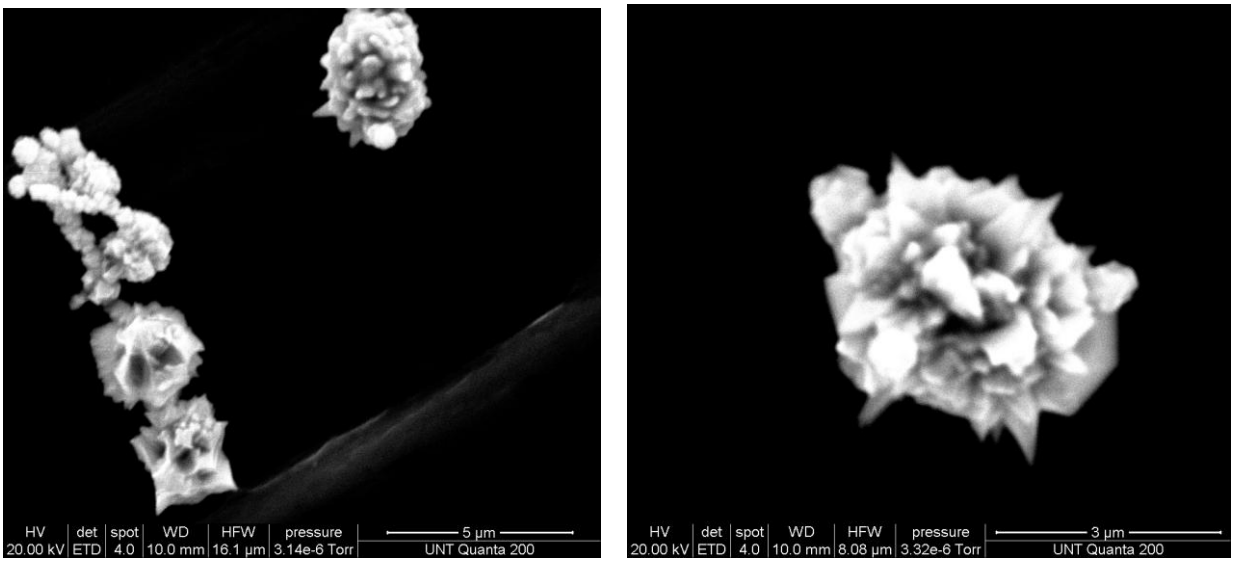

a b

Figures 22 a, b. SEM images of Ni particles.

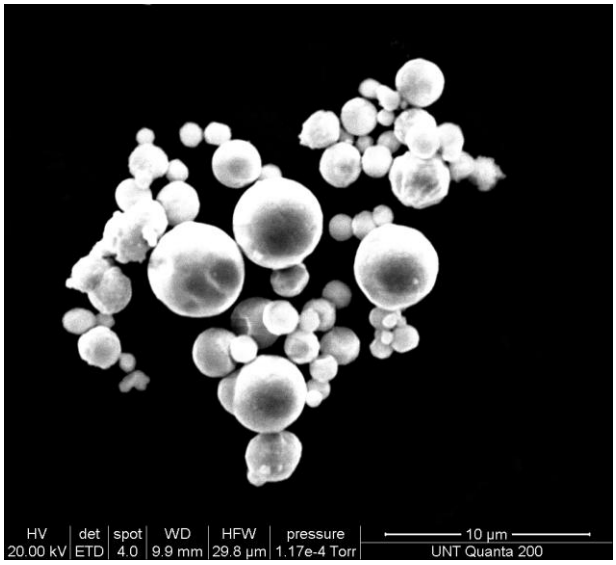

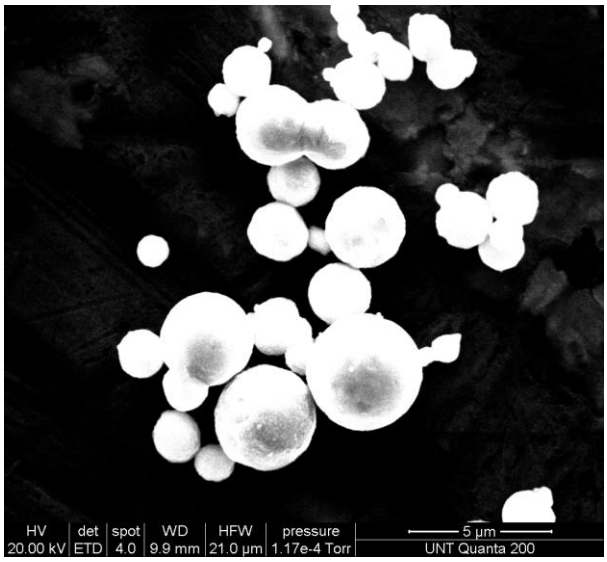

a b

Figures 23 a, b. SEM image of Al particles.

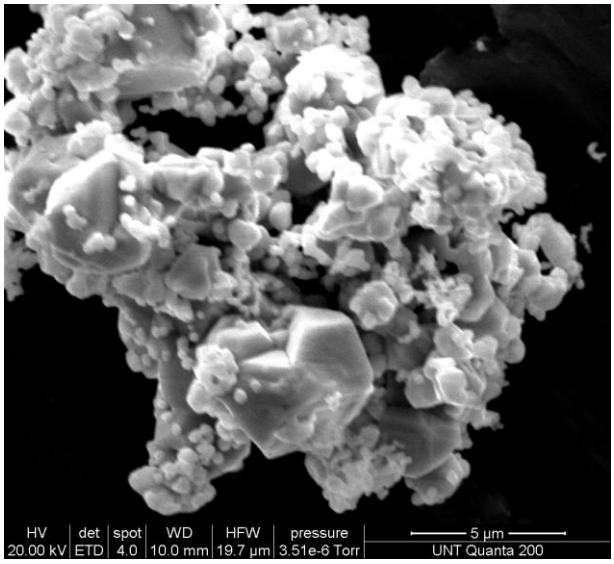

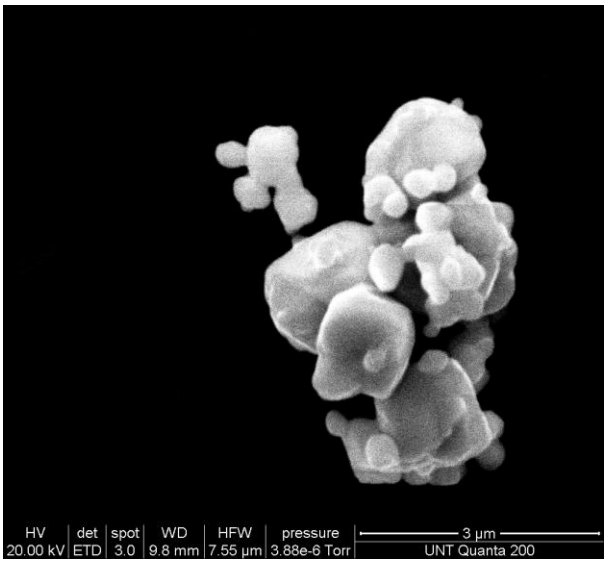

a b

Figures 24 a, b. SEM images of Ag particles.

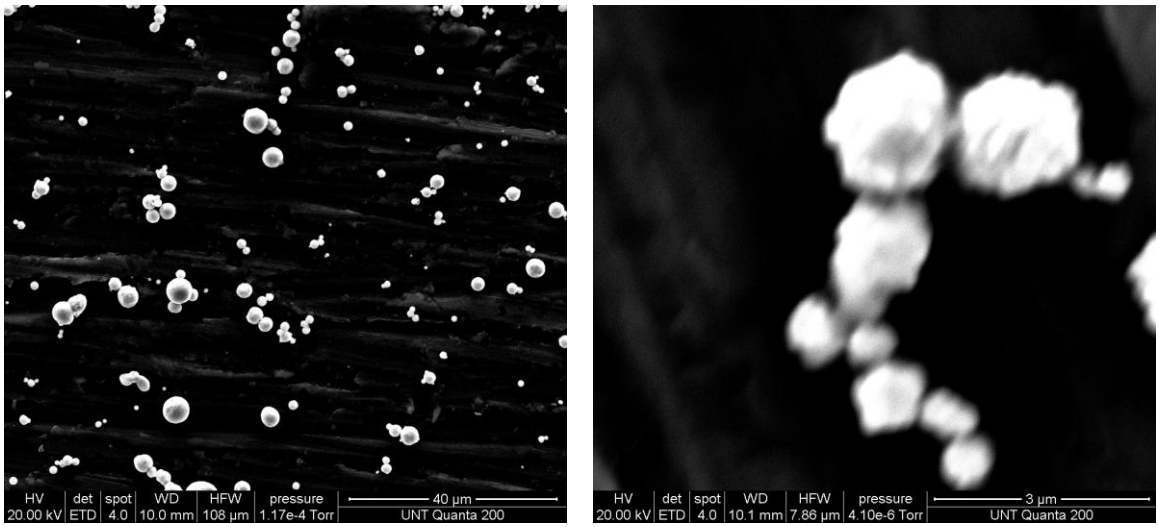

a b

Figures 25 a, b. SEM images of Zn particles.

4.2 Thickness of the Coatings

The Image J software which was used for determining the average particle size of the metal powders was as well used for determining the thickness of the coatings as well. As explained in the section 4.1.2 the software allows assigning a value of length to each pixel by relating the amount of pixels contained in the micrometric bar of each image (in this case the optical micrograph) and then the coating thickness can be calculated directly. 25 values of thickness were taken in each case and the average thickness of each coating was calculated.

The average thickness of the coatings is specified in Table 6 with their respective standard deviations mentioned in brackets.

Coating Composition	Thickness mm		
	Cured at 30 ^{o}C	Cured at 70 ^{o}C	Cured at 80 ^{o}C
Unmodified Epoxy	0.81 (0.05)	1.05 (0.02)	0.75 (0.01)
Epoxy + 12 FPEK	1.36 (0.01)	0.86 (0.02)	0.93 (0.02)
Epoxy + 12 FPEK + Ni	0.89 (0.02)	1.03 (0.02)	0.88 (0.01)
Epoxy + 12 FPEK + Al	0.95 (0.01)	0.84 (0.01)	0.77 (0.02)
Epoxy + 12 FPEK + Ag	1.03 (0.01)	0.76 (0.02)	1.22 (0.01)
Epoxy + 12 FPEK + Zn	0.8 (0.03)	1.35 (0.01)	1.29 (0.01)

Table 6. Average thickness of the coatings along with their respective standard deviations.

4.3 Pin on Disc Friction

It can be clearly observed from Figures 26 – 32 that the friction increased as the number of revolutions increased from 500 to 5000 irrespective of the curing temperature. To explain this, let us consider the first case where samples were cured at 30 ^{o}C. The friction of most of the coatings (except the epoxy + 12 FPEK + Al sample) cured at 30 ^{o}C was constant upto 500 revolutions and only after 500 revolutions the coating at the testing surface got worn out completely (Unmodified epoxy sample at 600 revolutions, epoxy + 12 FPEK sample at 2400 revolutions, epoxy + 12 FPEK + Ni sample at 400 revolutions, epoxy + 12 FPEK + Ag sample at 3000 revolutions, and epoxy + 12 FPEK + Zn sample at 600 revolutions) and the pin touched the steel substrate and at this point there occurs a sharp increase in friction (Figure 32) resulting in an increase in friction when tested upto 5000 revolutions. Second case is the set of samples cured at 70 ^{o}C. From Figure 33, the sample containing epoxy + 12 FPEK + Al

and epoxy + 12 FPEK samples got worn out after 500 revolutions (3200 revolutions and 2300 revolutions respectively). But all other samples worn out before 500 revolutions. The friction of unmodified epoxy sample increased gradually which accounts for less friction compared to samples containing Ni, Ag and Zn (Figure 27). The last case is the set of samples cured at 80 ^{o}C. From Figure 34, only the unmodified epoxy sample and the epoxy + 12 FPEK sample got worn out after 500 revolutions (3100 revolutions and 1500 revolutions respectively) and all other samples got worn out before 500 revolutions which is reason for less friction of the unmodified epoxy sample and the epoxy + 12 FPEK sample compared to others (Figures 28 and 31). In most of the cases, it can be observed that friction decreases with the addition of 12 FPEK to the epoxy phase.

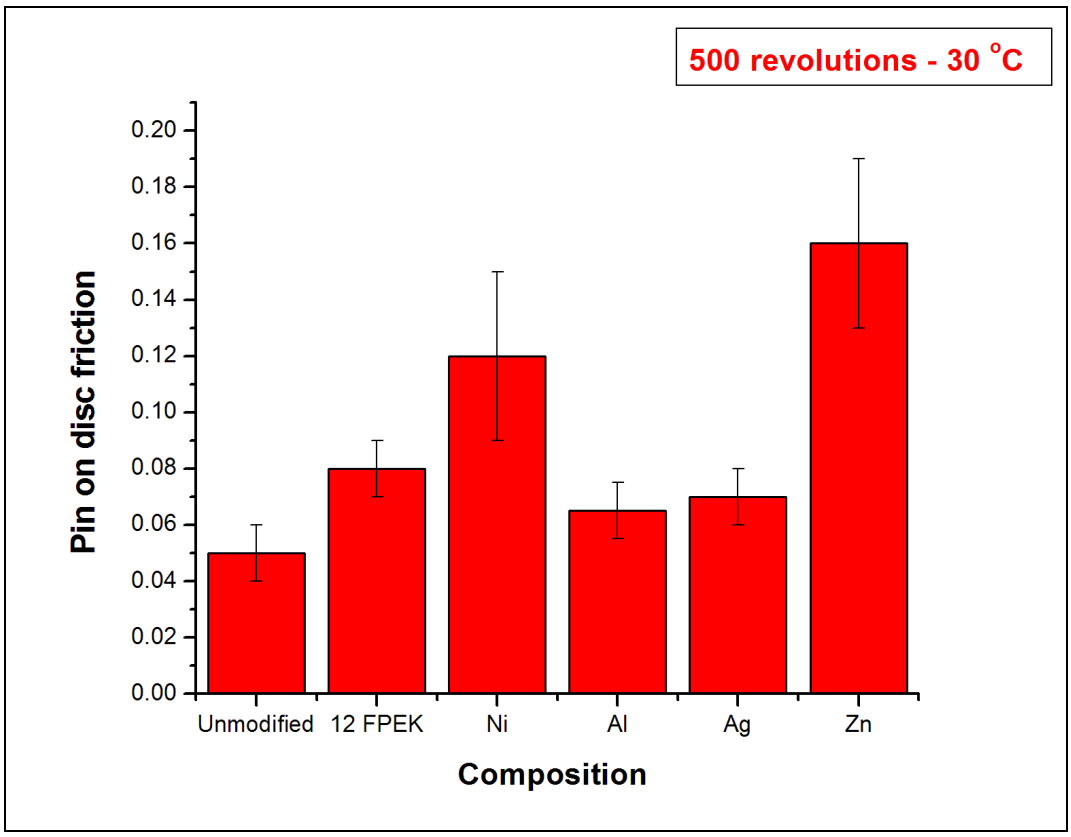

Figure 26. Pin on disc friction after 500 revolutions of samples cured at 30 ^{o}C.

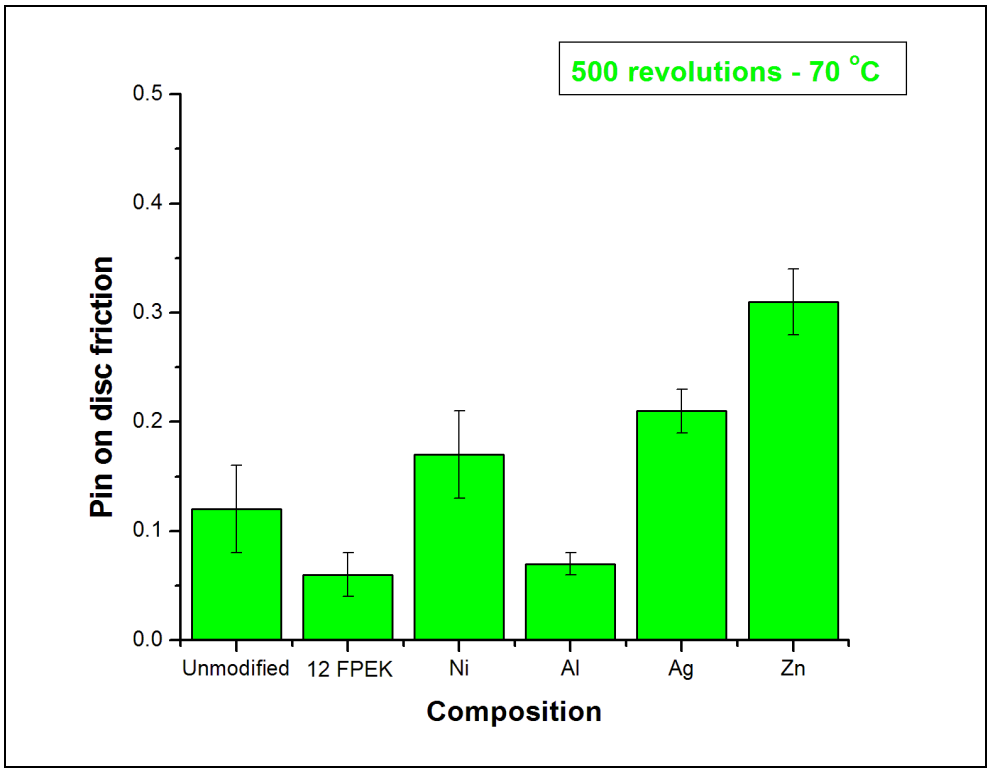

Figure 27. Pin on disc friction after 500 revolutions of samples cured at 70 °C.

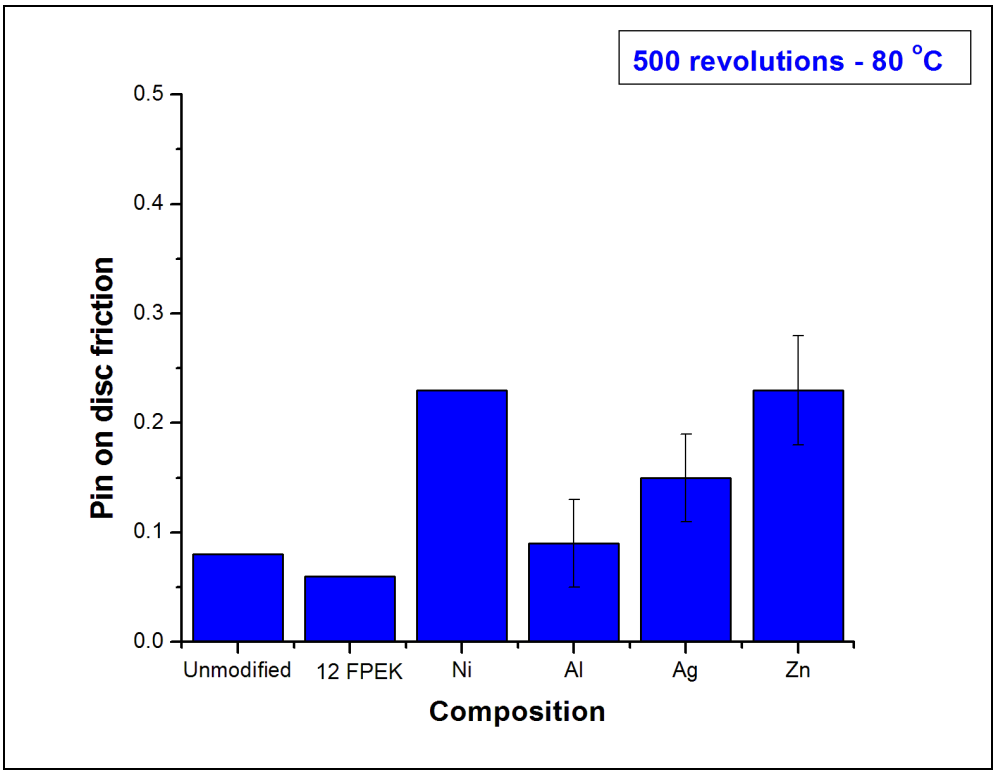

Figure 28. Pin on disc friction after 500 revolutions of samples cured at 80 °C.

From Figure 29, it is evident that there is a significant decrease in friction with the addition of 12 FPEK to plain epoxy. This can be explained from the fact that 12 FPEK seeks the free surface due to its low surface energy and phase inversion occurs in small domains. Similar result was observed by Haley during bulk modification of epoxy with 12 FPEK [31]. With the addition of metal powders the friction increases which is obvious as metal powders were added in powder form. But the friction is still less compared to the pure epoxy system. This is because when cured slowly at 30 ^{o}C, the difference in densities plays a very important role. As 12 FPEK has the least density it moves to the free surface and the metal particles being heavy sink to the bottom of the coating and there exists a softer matrix of epoxy below the accumulated 12 FPEK. So the average friction that results after 5000 revolutions for the samples containing metal powders is a total result of epoxy + 12 FPEK + metal powder.

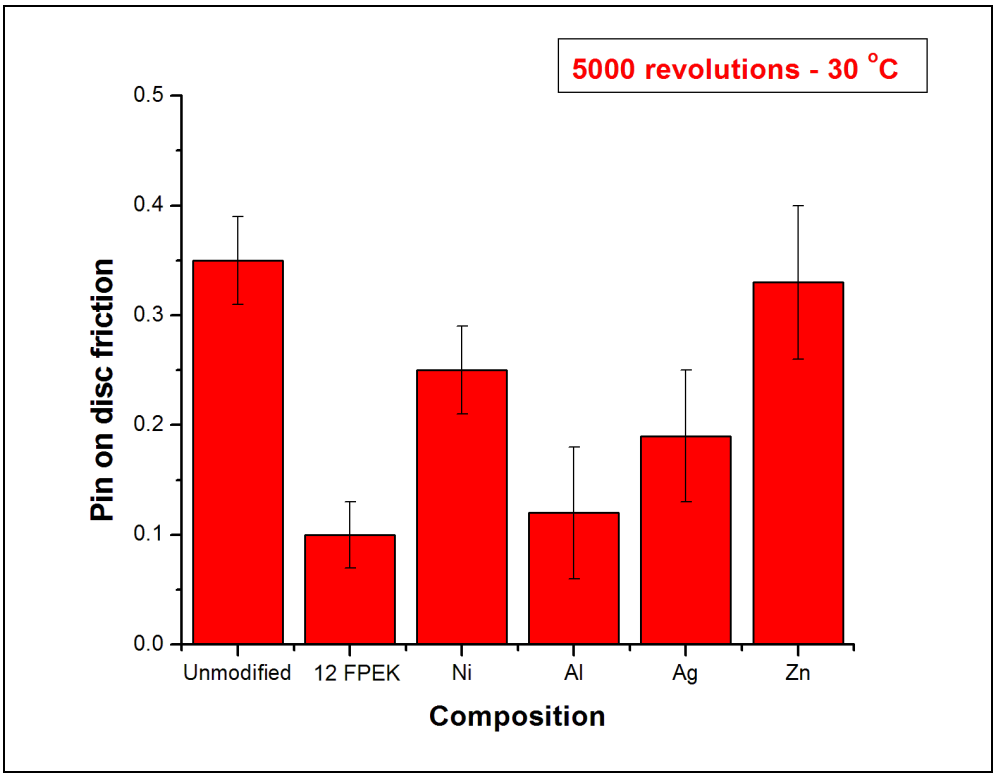

Figure 29. Pin on disc friction after 5000 revolutions of samples cured at 30 ^{o}C.

From figure 30, it is clear that with the addition of 12 FPEK the coating still shows less friction compared to the unmodified epoxy system even when cured at 70 ^{o}C but the samples containing metal powders show an increase in friction. This is because when cured at 70 ^{o}C the rate of curing increases significantly, hence the cross linking reaction is favored than the phase separation. Therefore the 12 FPEK doesn't get sufficient time to move to the free surface and occupy the entire free surface. Hence, a mixture of 12 FPEK and epoxy phases exist at the free surface in the case of epoxy + 12 FPEK system and some amount of metal powders get entrapped near the free surface which results in an increase in friction. The increase in friction with the addition of metal powders is also because of the morphology of the particles. As Ni is flaky; Ag and Zn are irregular particles the friction increases (Figures 22 a, b; 24 a, b and 25 a, b). However, since Al particles are spherical (Figure 23 a, b) the sample containing Al shows less friction compared to samples containing Ni, Ag, and Zn. The highest friction of the sample containing Zn is due to the existence of ZnO phase along with epoxy, 12 FPEK and Zn.

The same reason accounts for the increase in friction in the case of curing the samples at 80 ^{o}C where the rate of curing is higher than that of the case of curing at 70 ^{o}C.

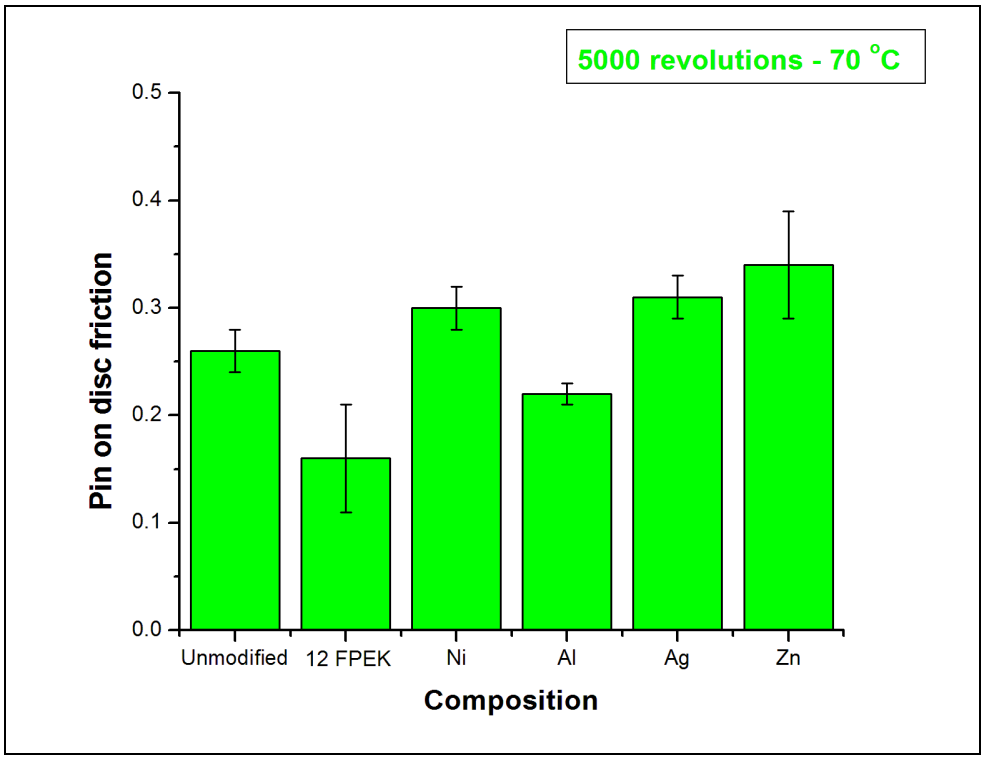

Figure 30. Pin on disc friction after 5000 revolutions of samples cured at 70 °C.

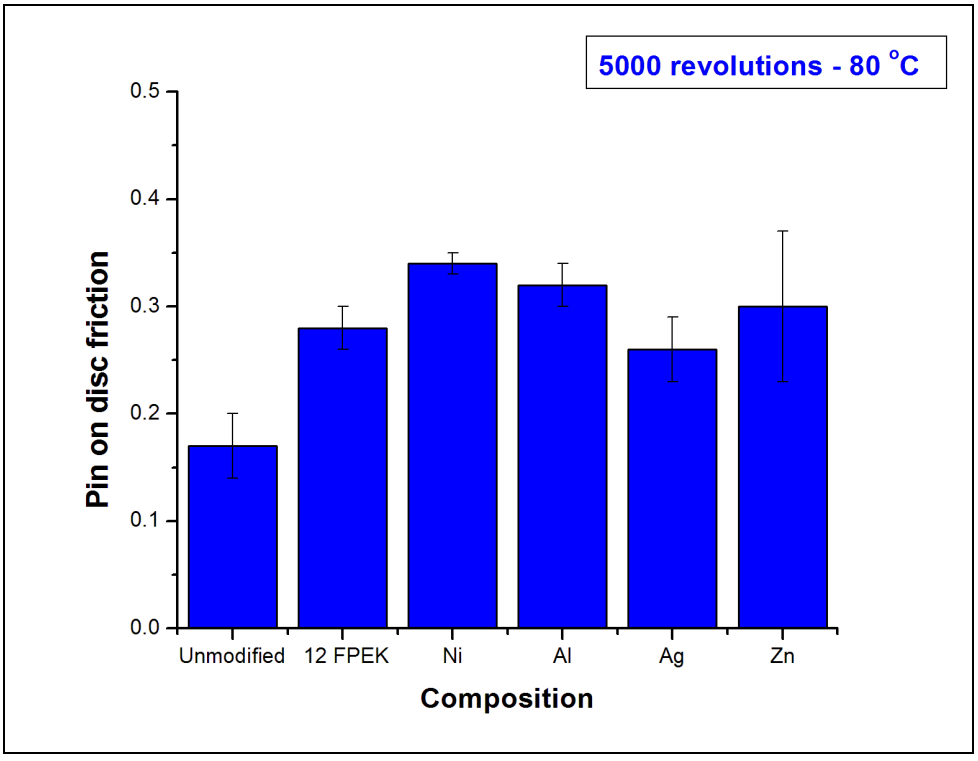

Figure 31. Pin on disc friction after 5000 revolutions of samples cured at 80 °C.

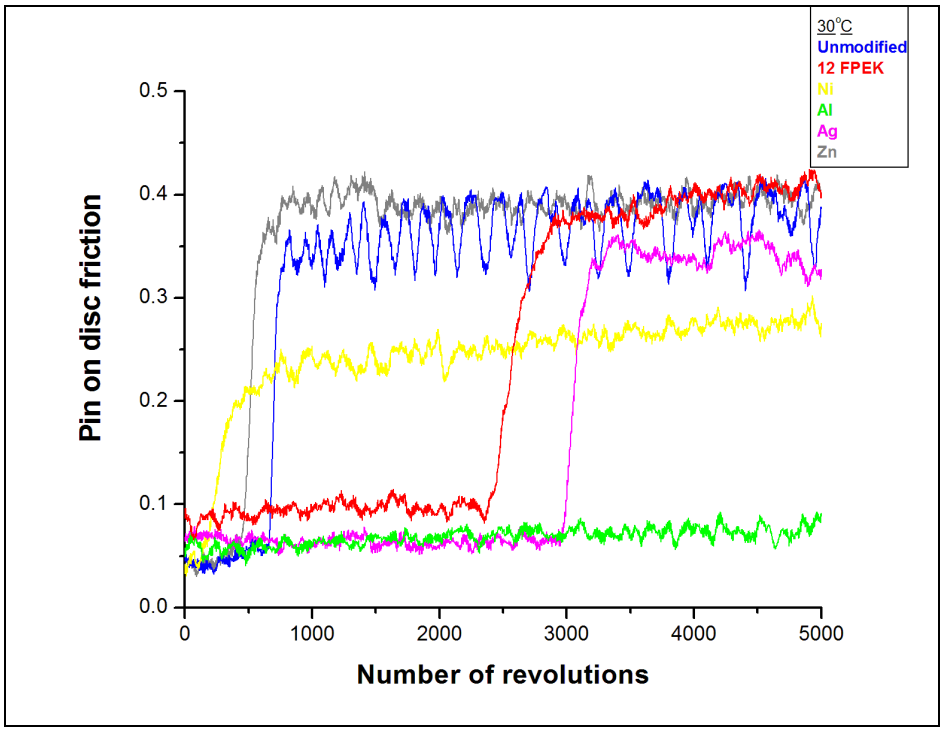

Figure 32. Pin on disc friction vs number of revolutions of samples cured at 30 °C.

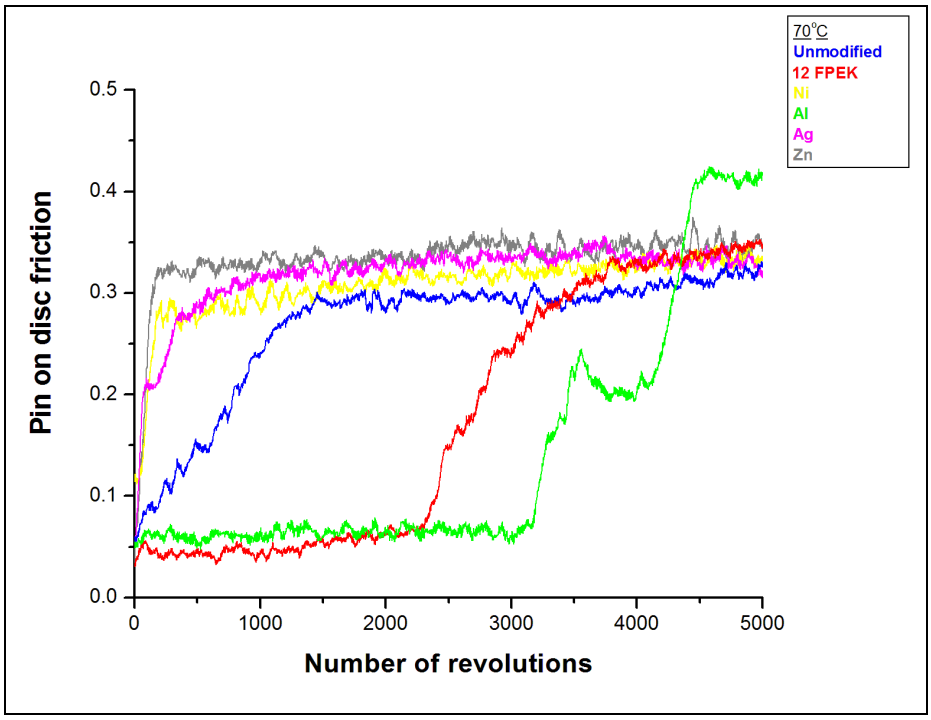

Figure 33. Pin on disc friction vs number of revolutions of samples cured at 70 °C.

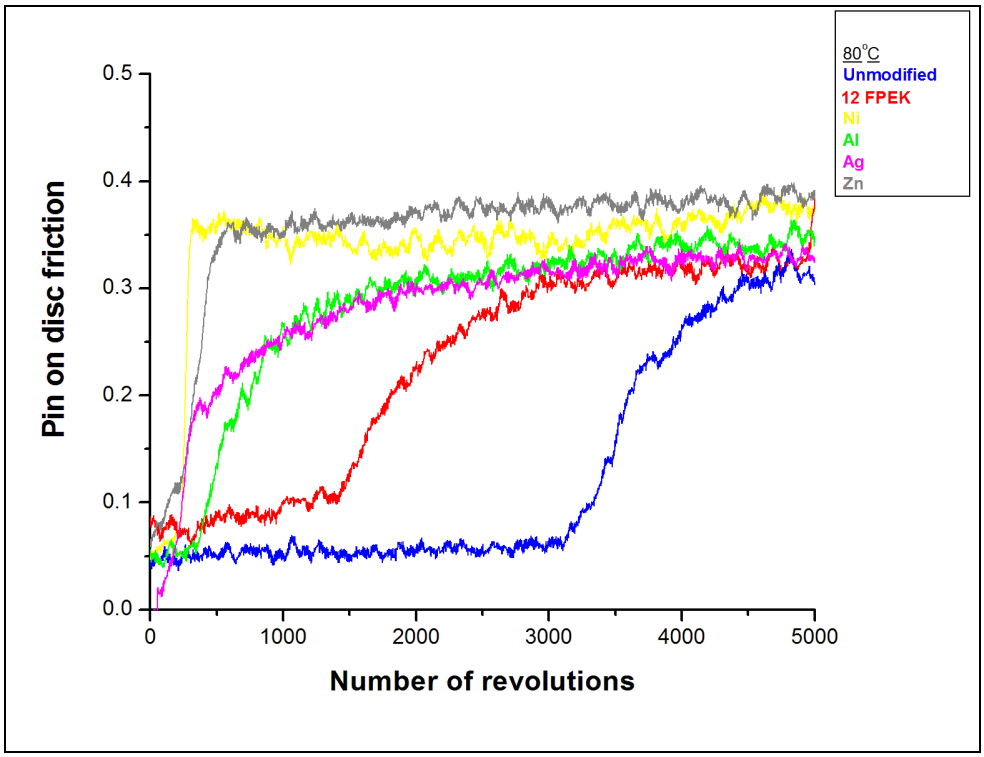

Figure 34. Pin on disc friction vs number of revolutions of samples cured at 80 ^{o}C.

4.4 Wear

From Figure 35 it can be observed that with the addition of 12 FPEK and metal powders the wear rate decreases. Samples containing metal powders show less wear rate because epoxy and 12 FPEK are softer phases and the metallic phase is a harder phase. Samples containing Ni, Ag, and Zn show higher wear rates compared to sample containing Al because of their morphology as explained in the earlier section. Because of the irregular morphology, there exists stress at the interface of these particles and hence an increase in wear rate. The least wear rate for the sample containing Al can be explained from Figure 32 where the same sample shows the least friction.

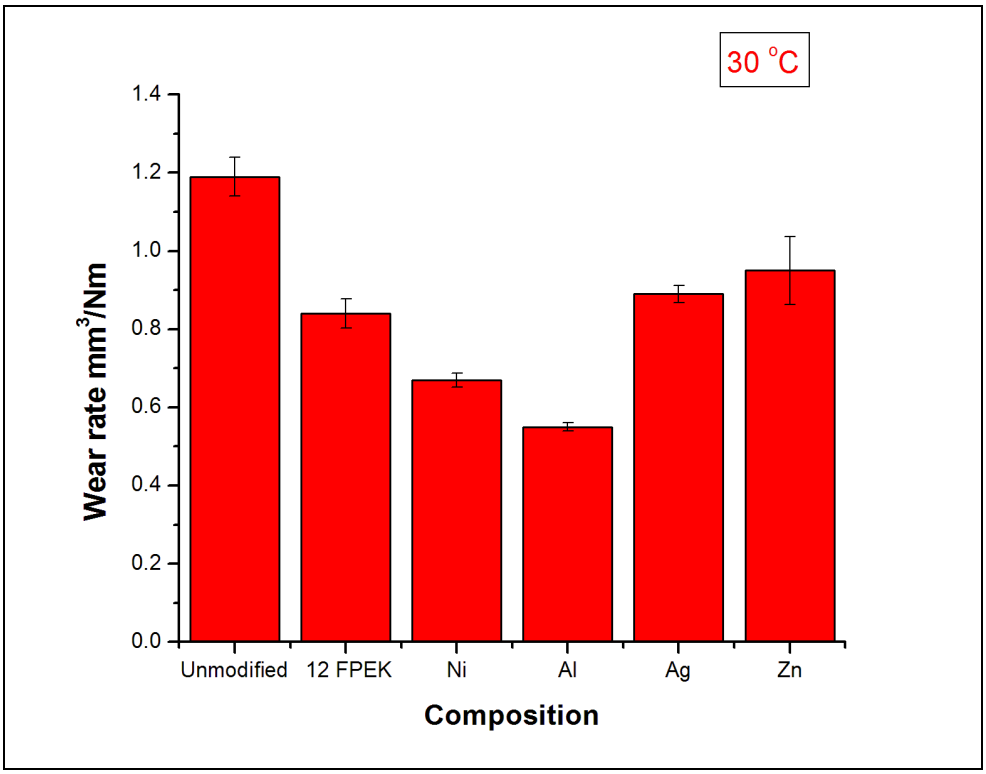

Figure 35. Wear rate of the samples cured at 30 ^{o}C.

In the case of curing at 70 ^{o}C and 80 ^{o}C, as the cross linking reaction competes with the phase separation and is favored, these systems tend to show higher wear rates with the addition of the metal powders. The high wear rate of sample containing Zn can be related to the same fact of existence of ZnO phase. Samples containing Ni and Al show high wear rate when cured at 80 ^{o}C. This is because the test surface of the coating gets worn out as early as 250 revolutions in the case of sample containing Ni and before 1000 revolutions in the case of sample containing Al.

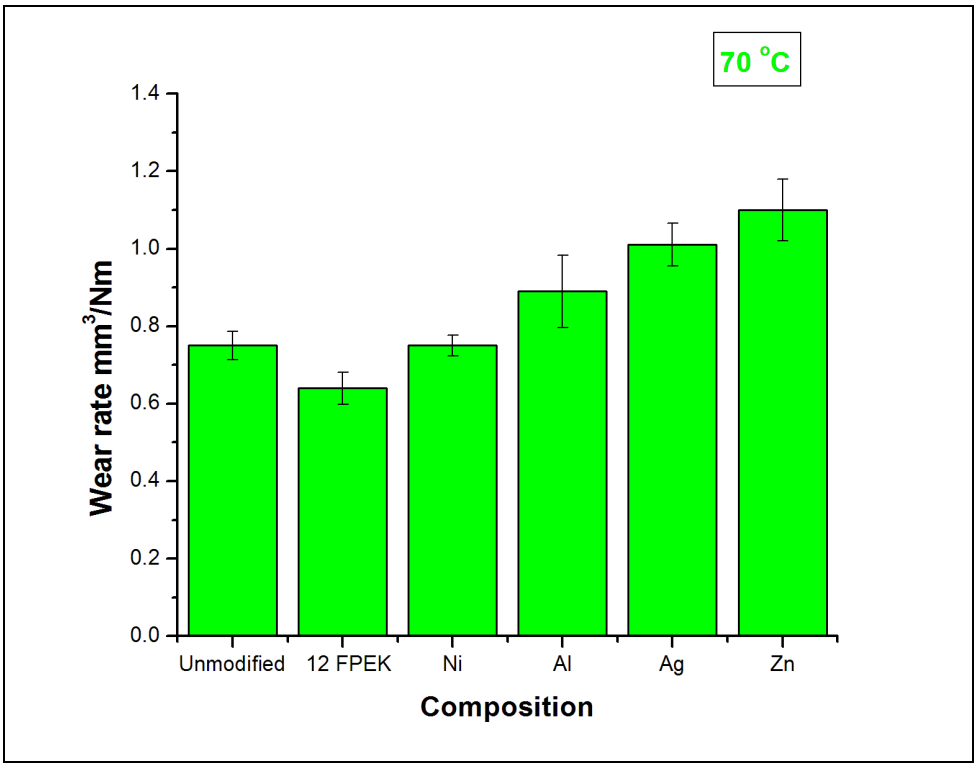

Figure 36. Wear rate of the samples cured at 70 °C.

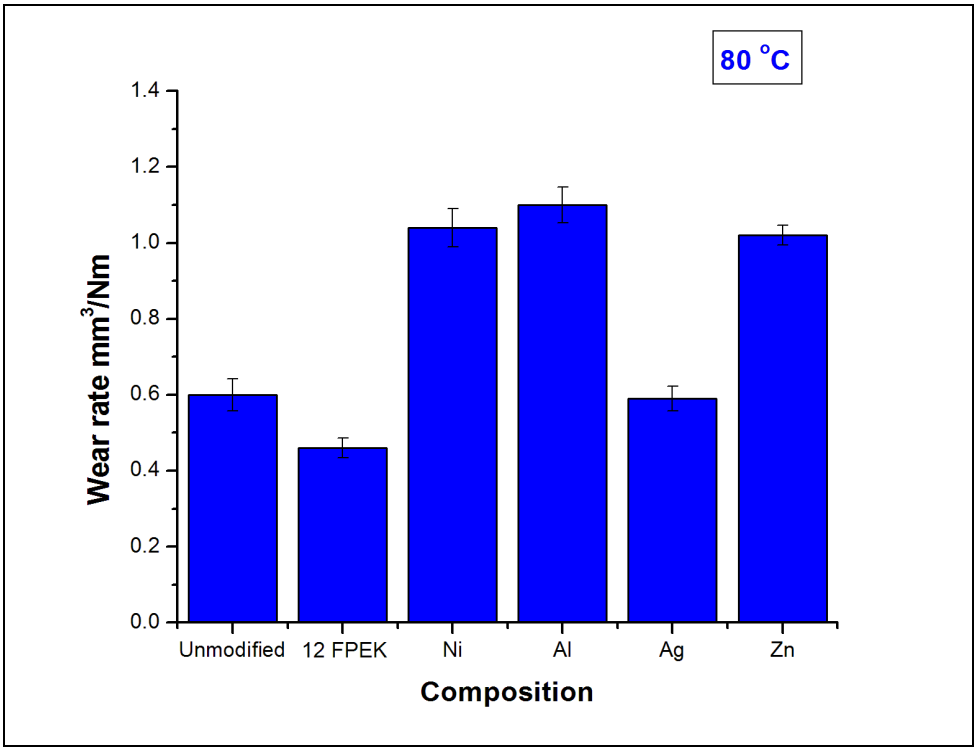

Figure 37. Wear rate of the samples cured at 80 °C.

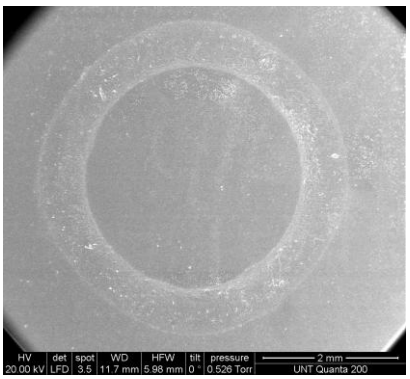

a. Unmodified Epoxy

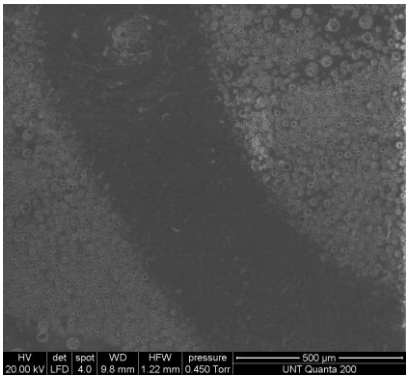

b. Epoxy + 12 FPEK

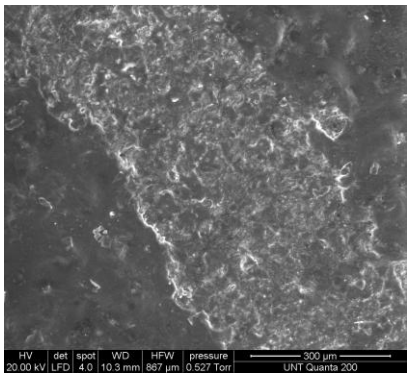

c. Epoxy + 12 FPEK + Ni

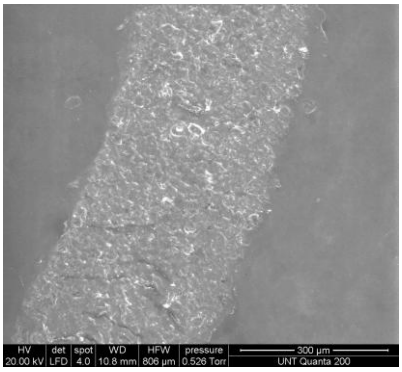

d. Epoxy + 12 FPEK + Al

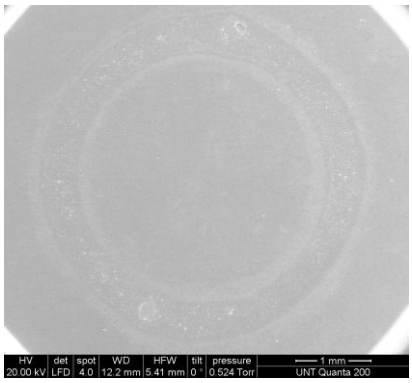

e. Epoxy + 12 FPEK + Ag

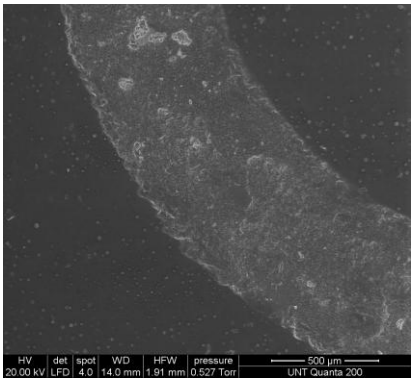

f. Epoxy + 12 FPEK + Zn

Figure 38. SEM images of the wear tracks of samples cured at 30 ^{o}C.

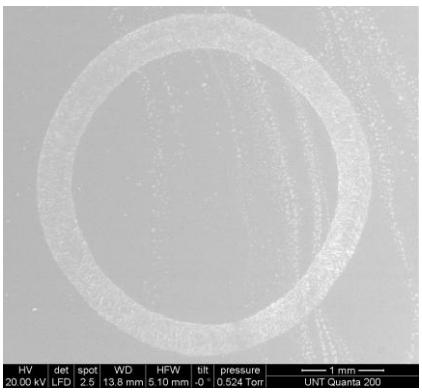

a. Unmodified Epoxy

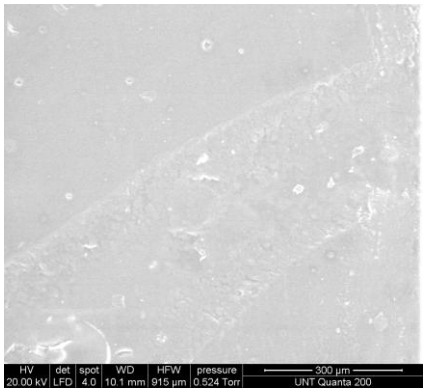

b. Epoxy + 12 FPEK

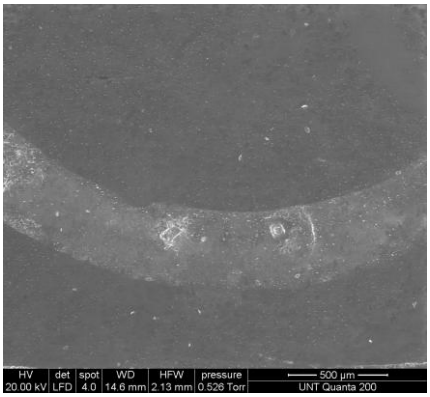

c. Epoxy + 12 FPEK + Ni

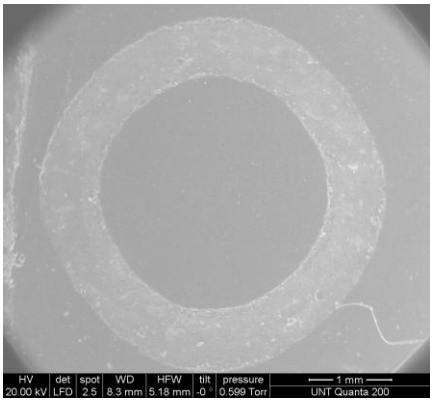

d. Epoxy + 12 FPEK + Al

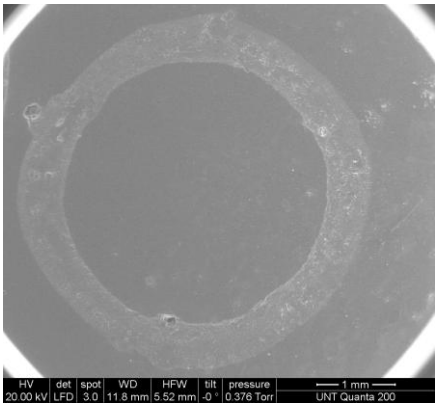

e. Epoxy + 12 FPEK + Ag

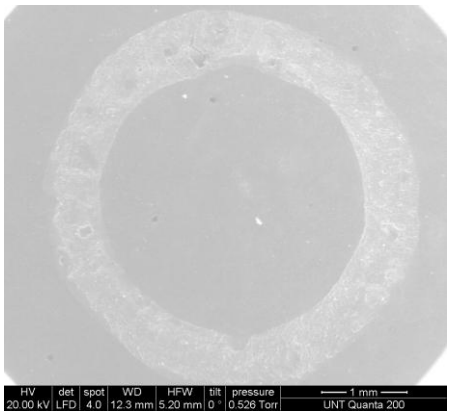

f. Epoxy + 12 FPEK + Zn

Figure 39. SEM images of the wear tracks of samples cured at 70 ^{o}C.

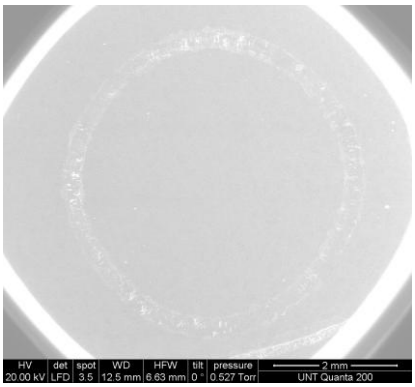

a. Unmodified Epoxy

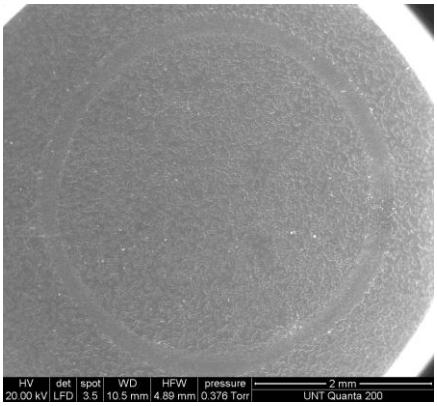

b. Epoxy + 12 FPEK

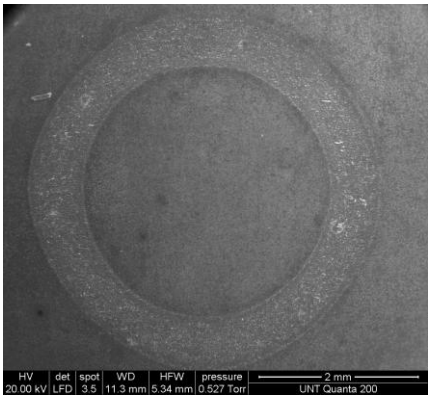

c. Epoxy + 12 FPEK + Ni

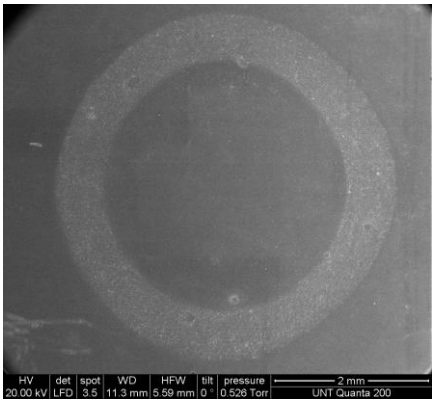

d. Epoxy + 12 FPEK + Al

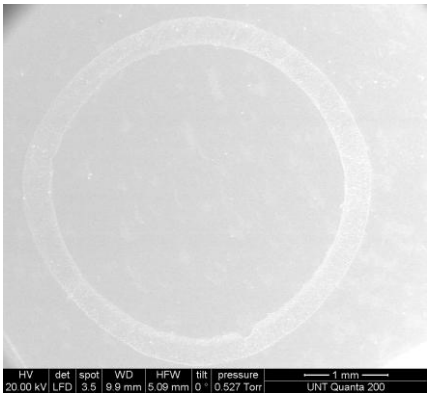

e. Epoxy + 12 FPEK + Ag

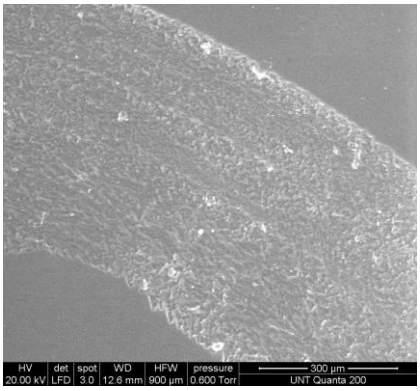

f. Epoxy + 12 FPEK + Zn

Figure 40. SEM images of the wear tracks of samples cured at 80 ^{o}C.

4.5 Contact Angles and Surface Energies

Contact angles increase with the addition of modifiers and with an increase in curing temperature (Table 64). To explain this, let us consider the first case of 30 ^{o}C curing temperature. Here, with the addition of 12 FPEK the contact angle (θ) increases by 33^{o} due to the hydrophobic nature of 12 FPEK as expected. Let us now consider the case of 70 ^{o}C curing temperature. In case of pure epoxy, the temperature increase (30 ^{o}C to 70 ^{o}C) leads to an increase in θ by 63.4 %. Similarly, in case of epoxy + 12 FPEK, the temperature increase (30 ^{o}C to 70 ^{o}C) leads to an increase in θ by 24.3 %. This means that at higher temperature (70 ^{o}C) the presence of 12 FPEK still results in an increase in θ while epoxy as the main component also increases θ. The result is a θ increase – but clearly this increase is less than that for pure epoxy which is because of the existence of two phases at the free surface in cured epoxy + 12 FPEK. Also the absolute difference between the θ for pure epoxy and θ for epoxy + 12 FPEK is 25^{o} at 70 ^{o}C which can be attributed to the less FPEK migrating to the free surface unlike the case of 30 ^{o}C where the 12 FPEK occupies the entire free surface.

Now let us consider the 80 ^{o}C curing temperature. The explanation above can be extended here as well. The difference between the θ for pure epoxy and that θ for epoxy + 12 FPEK is here 5^{o} increase only which is because of very less FPEK migration to the free surface in the case of 80 ^{o}C. Also, addition of 12 FPEK still increases the θ (from 30 ^{o}C to 80 ^{o}C) but by only 20.3 % which is less since there is less FPEK at the surface.

Composition	Curing temperature °C	Contact Angle °	
		Water	Diiodomethane
Steel	30 °C	90	53
Unmodified Epoxy		41	52
Epoxy + 12 FPEK		74	62
Epoxy + 12 FPEK + Ni		70	58
Epoxy + 12 FPEK + Al		82	57
Epoxy + 12 FPEK + Ag		85	63
Epoxy + 12 FPEK + Zn		47	70
Steel	70 °C	90	53
Unmodified Epoxy		67	41
Epoxy + 12 FPEK		92	45
Epoxy + 12 FPEK + Ni		88	50
Epoxy + 12 FPEK + Al		83	55
Epoxy + 12 FPEK + Ag		97	45
Epoxy + 12 FPEK + Zn		72	46
Steel	80 °C	90	53
Unmodified Epoxy		84	48
Epoxy + 12 FPEK		89	52
Epoxy + 12 FPEK + Ni		96	49
Epoxy + 12 FPEK + Al		85	59
Epoxy + 12 FPEK + Ag		83	65
Epoxy + 12 FPEK + Zn		85	53

Table 7. Contact angles of all the samples.

Fluorine – containing polymers have low surface free energy, low tendency for water uptake, and high water repellence [9, 81,84 – 86]. Therefore, the addition of 12 FPEK to the epoxy should decrease the surface energy significantly. And the expected trend was followed by the samples as shown in Figures 41 – 43. The decrease in surface tension decreases with the increase in curing temperature. The reason for this is the same explanation provided in the earlier sections: as the curing temperature increases the phase separation reaction decreases and the cross linking reaction is favored. Therefore, if we consider the case of curing at 30 ^{o}C, the 12 FPEK phase is present at the entire free surface. Hence a steep decrease in surface energy and it is almost constant, as in all the other cases the 12 FPEK migrated to the free surface. But in case of sample containing Zn, the surface energy increases which supports its high friction reported in section 4.3 (Figure 26). Considering the case of curing at 70 ^{o}C, though the surface energy decreases but the step of decrease is not as steep as the earlier case of 30 ^{o}C curing temperature. The step decreases much more in the case of curing at 80 ^{o}C. The surface energy of the sample containing Zn is much higher in the both of cases of 70 ^{o}C and 80 ^{o}C curing. This is because of the presence of any trapped Zn and ZnO particles and their morphology.

Sample	Dispersive Component mN/m	Polar Component mN/m	Surface Energy mN/m
Unmodified Epoxy	34.43	29.22	63.65
Epoxy + 12 FPEK	34.55	5.81	40.36
Epoxy + 12 FPEK + Ni	36.03	3.05	39.08
Epoxy + 12 FPEK + Al	30.95	8.08	39.03
Epoxy + 12 FPEK + Ag	30.79	7.22	38.01
Epoxy + 12 FPEK + Zn	25.82	29.53	55.35

Table 8. Surface energies and their components of systems cured at 30 ^{o}C.

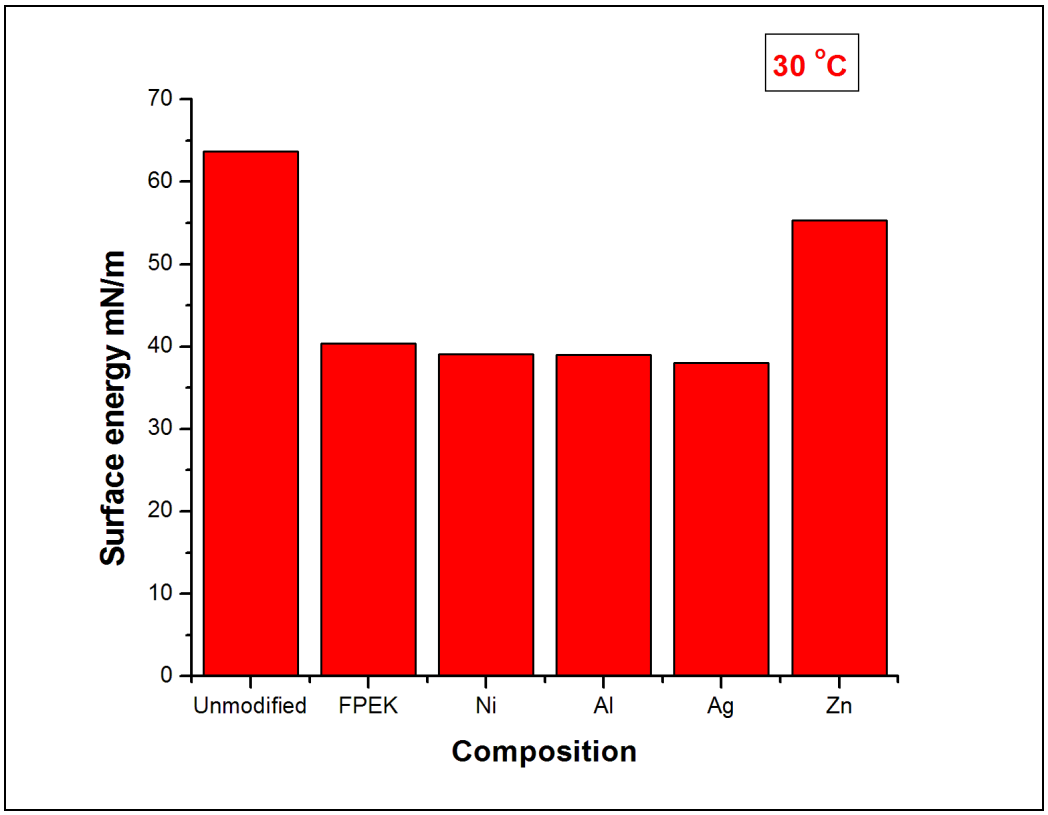

Figure 41. Surface energies of samples cured at 30 ^{o}C.

Sample	Dispersive Component mN/m	Polar Component mN/m	Surface Energy mN/m
Unmodified Epoxy	37.78	16.52	54.31
Epoxy + 12 FPEK	38.3	3.6	41.9
Epoxy + 12 FPEK + Ni	31.2	8.59	39.79
Epoxy + 12 FPEK + Al	32.92	8.13	41.05
Epoxy + 12 FPEK + Ag	29.93	9.85	39.78
Epoxy + 12 FPEK + Zn	37.4	12.32	49.72

Table 9. Surface energies and their components of systems cured at 70 ^{o}C

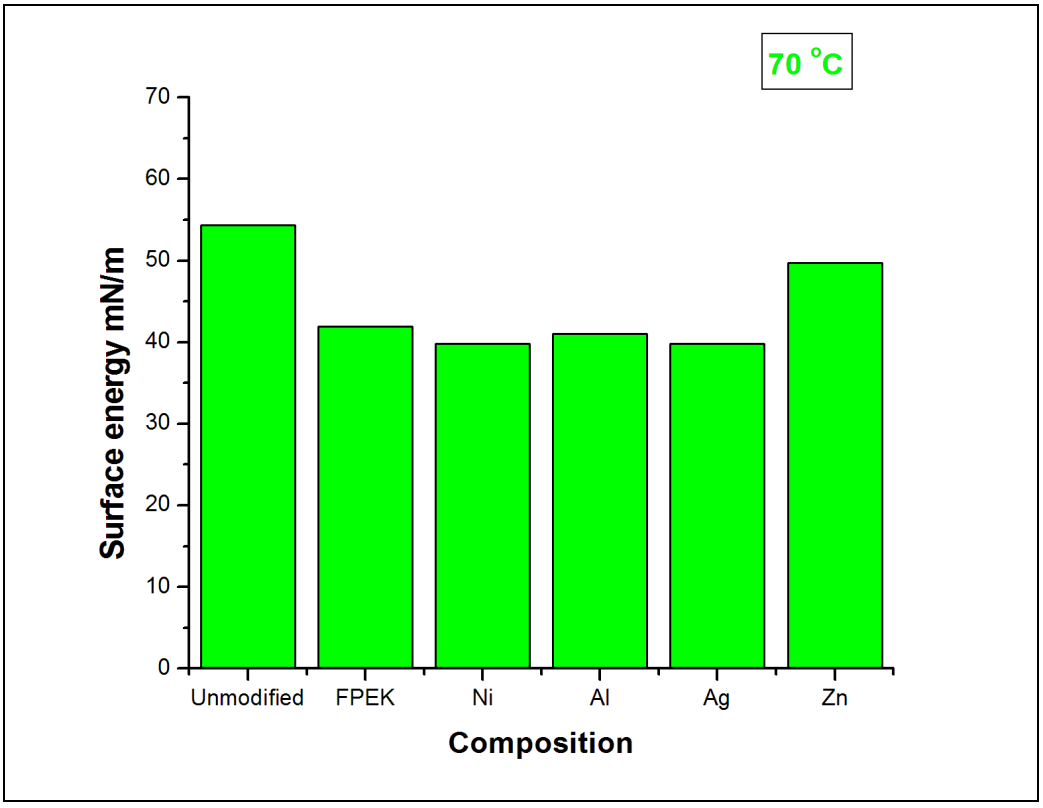

Figure 42. Surface energies of samples cured at 70 ^{o}C

Sample	Dispersive Component mN/m	Polar Component mN/m	Surface Energy mN/m
Unmodified Epoxy	36.24	6.49	48.73
Epoxy + 12 FPEK	29.54	15.64	45.18
Epoxy + 12 FPEK + Ni	35.28	6.13	41.41
Epoxy + 12 FPEK + Al	32.07	9.26	41.31
Epoxy + 12 FPEK + Ag	32.82	6	40.06
Epoxy + 12 FPEK + Zn	33.73	8.01	55.35

Table 10. Surface energies and their components of systems cured at 80 ^{o}C.

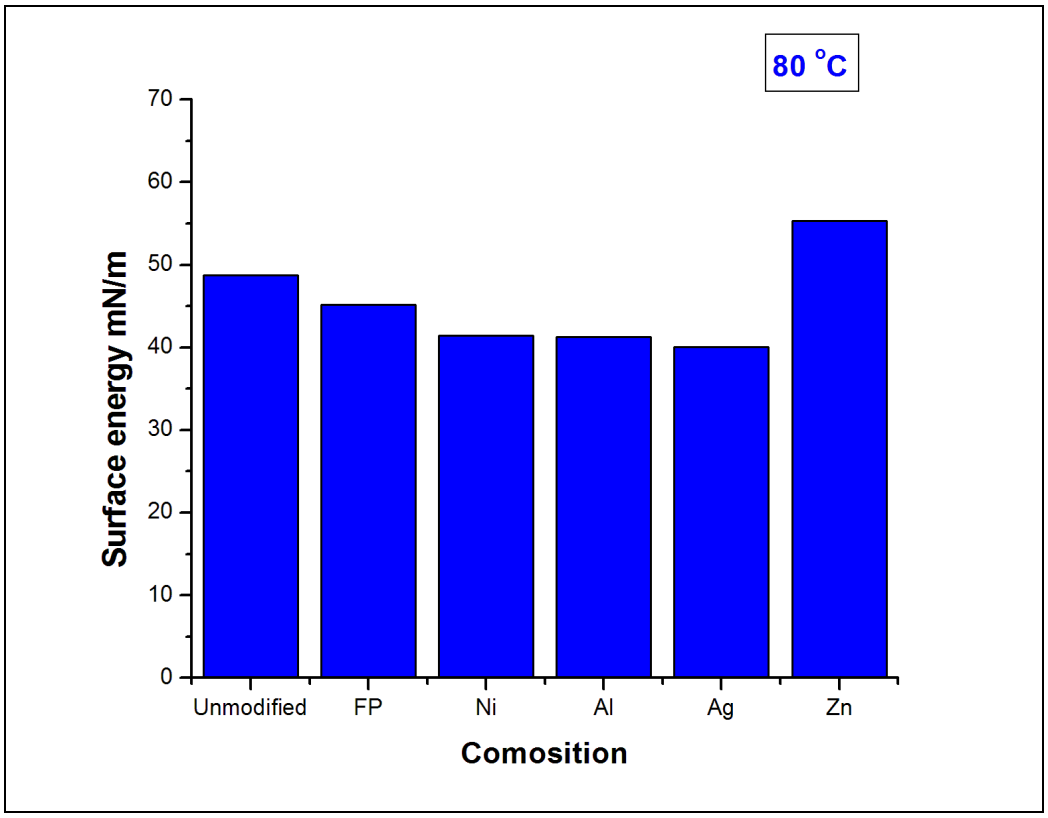

Figure 43. Surface energies of samples cured at 80 ^{o}C.

4.6 Surface Roughness

Surface roughness was determined for three samples cured at the three curing temperatures (30 ^{o}C, 70 ^{o}C, 80 ^{o}C) along with the pure epoxy sample cured at 30 ^{o}C, just to analyze the change in surface roughness with the increase in curing temperature. The center-line average (R_a) and the root mean square average (R_q) have been reported.

The unmodified epoxy sample exhibits lowest surface roughness and as the modifiers (12 FPEK and metal powders are added) the surface roughness increases. With the increase in curing temperature the surface roughness increases furthermore. This again goes back to the same explanation that when time is allowed for the modified epoxy systems to cure slowly, phase separation occurs and the entire free surface can be occupied with one phase – 12 FPEK.

Coating Composition	**R_a nm**	**R_q nm**
Unmodified Epoxy	58.11	73.83
Epoxy + 12 FPEK + Ni (cured at 30 ^{o}C)	124.35	157.01
Epoxy + 12 FPEK + Ni (cured at 70 ^{o}C)	163.97	198.30
Epoxy + 12 FPEK + Ni (cured at 80 ^{o}C)	254.20	312.76

Table 11. Surface roughness of unmodified epoxy cured at 30 ^{o}C and samples containing Ni cured at 30 ^{o}C, 70 ^{o}C and 80 ^{o}C

4.7 FTIR – ATR Measurements

Four samples: epoxy + 12 FPEK (cured at 30 ^{o}C) and epoxy + 12 FPEK + Ni (cured at 30 ^{o}C, 70 ^{o}C and 80 ^{o}C) were tested for surface composition using FTIR – ATR. The reason for choosing epoxy + 12 FPEK sample for this test was this sample had 12 FPEK at the entire free surface. And since characteristic absorbance literature for 12 FPEK was not available, it was pertinent to obtain the ATR for the 12 FPEK sample and then compare the results of the rest of the samples with the 12 FPEK sample.

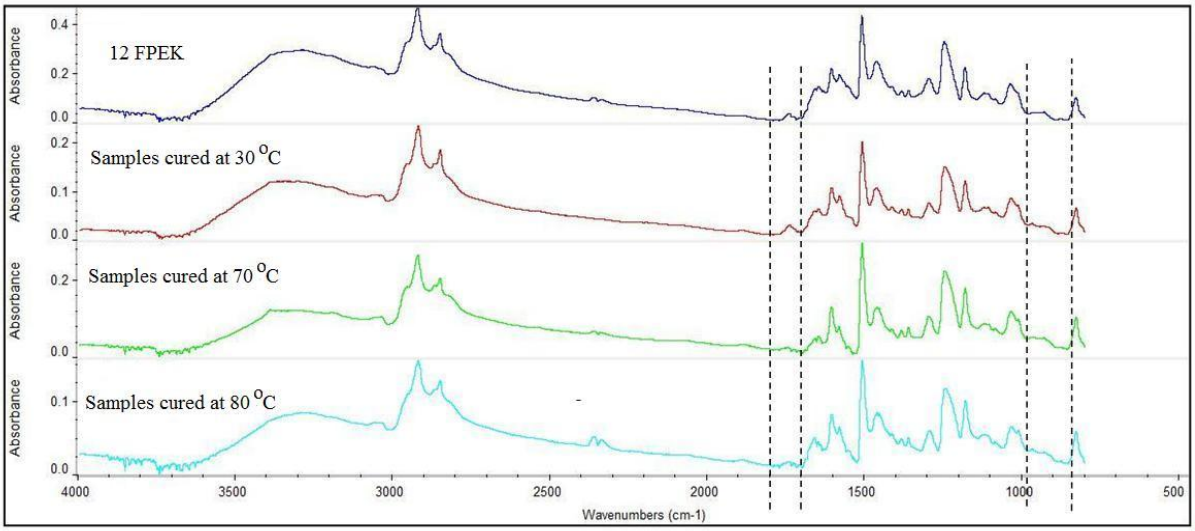

Figure 44. ATR graph of three samples with Ni cured at different curing temperatures compared with the 12 FPEK sample.

There are few new bands which appear when the curing temperature increases. In Figure 44, the band at ~ 1750 cm^{-1} refers to carbonyl group [87] and such a group is present only in 12 FPEK among the materials used. Therefore this band refers to the 12 FPEK phase. The band slowly disappears as the temperature increases which means that the 12 FPEK phase is slowly decreasing as the temperature increases. At the same time, there are new characteristic bands forming between 820 cm^{-1} and 980 cm^{-1} as the

temperature increases and these correspond to the DGEBA epoxy [88]. This means that as the temperature increases, there is a mixture of 12 FPEK and epoxy phases that coexist at the free surface. This supports the increasing trend of surface energy and friction with increasing curing temperature. The bands at 3300 cm^{-1} and 2900 – 3050 cm^{-1} correspond to the hydroxyl and C – H groups of DGEBA. There is no change in these peaks in all the four systems corresponding to the presence of DGEBA present under the 12 FPEK [88].

CHAPTER 5

CONCLUSIONS

DGEBA epoxy was modified using 12 FPEK and micro metal powders (Ni, AL, Ag, and Zn). Two curing agents were used (TETA and HMDA) and three different types of systems were synthesized, each system consisted of six compositions. Each system was coated onto ASTM A366 steel substrates of 1” X 2” dimensions and cured.

The morphology and composition of the metal powders was analyzed using SEM and XRD as the morphology and the phases that exist has an effect over the properties of the end coating.

The thickness of coatings was determined by cutting each sample into two halves (perpendicular to its length) and analyzing the cross section using an optical microscope.

Pin on disc test was used for determining the dynamic friction of the coatings. Friction after 500 revolutions and 5000 revolutions was determined. All the samples showed an increase in friction when the revolutions were increased from 500 to 5000. This is because most of the samples got worn out when tested uptil 5000 revolutions, therefore the pin touched the steel surface which resulted in an increase in friction as the friction reported is an average of all the friction values obtained during the test. Friction decreased with the addition of 12 FPEK to the epoxy as during curing the 12 FPEK migrates to the free surface since the surface energy of 12 FPEK is lower than that of pure epoxy. Sample containing Zn showed high friction in all the cases because of the presence of ZnO phase along with Zn phase. Also, the morphology of the Zn and ZnO particles was responsible for high friction. Sample containing Al showed least

friction when compared to the modified systems containing metal powders. This is because of the spherical morphology of Al particles which results in rolling friction. Friction of the samples increased as the curing temperature increased. This can be explained by the fact that at high temperatures, cross linking reaction competes with phase separation and is favored resulting in a mixture of epoxy and 12 FPEK phases at the free surface.

Wear rate was determined by determining the volume loss of the material after the pin on disc test (5000 revolutions). The volume loss was determined using the formula suggested by ASTM G99 standard. For this, the wear track width was calculated by examining the wear tracks under an SEM. Wear rate decreased with the addition of modifiers (12 FPEK and metal powders) in the case of curing at 30 ^{o}C. However, at higher curing temperatures the wear rate increased with the addition of modifiers especially by adding metal powders. This is because there is no sufficient time for the 12 FPEK to migrate to the free surface and the metal powders to sink down. As a result they got entrapped at random places in the coatings resulting in an increase in wear rate.

The contact angles (θ) were determined for two test liquids: a polar liquid (water) and an apolar liquid (diiodomethane) using a goniometer. θ increased with the addition of modifiers meaning that the hydrophobicity of the samples increased. The water contact angles increased significantly as the curing temperature increased. This is because at higher curing temperatures (70 ^{o}C and 80 ^{o}C) the presence of 12 FPEK still results in an increase in θ while epoxy as the main component also increases θ. Therefore the net result is an increase in θ.

Surface energies of the coatings were determined using Wu's equations (harmonic mean method) based on water and diiodomethane contact angles. When cured at 30 ^{o}C, surface energies decreased significantly with the addition of modifiers. But when the curing temperature was increased to 70 ^{o}C and 80 ^{o}C, the decrease of surface energies when compared to unmodified epoxy sample decreased because of the presence of two phases (epoxy and 12 FPEK) at the free surface. Sample containing Zn shows high surface energy which supports high friction for the same material.

Surface roughness of the coatings was determined using profilometry. The surface roughness of the samples increases with the increase in curing temperature. The reason for this is as same as mentioned earlier that at higher temperatures the cross linking reaction is favored.

Hence, with the addition of modifiers there was an increase in dynamic friction but the wear rate decreased and surface energy decreased as well. But this was in the case of 30 ^{o}C curing temperature only. When the curing temperature was increased to 70 ^{o}C and 80 ^{o}C, friction, wear rate and surface energy increased.

REFERENCE LIST

[1] J. I. DiStasio, *Epoxy Resin Technology: Development since 1979,* Noyes Data Corp, New Jersey, 1982.

[2] C. A. May, *Epoxy Resins: Chemistry and Technology,* 2nd ed., ed. C. A. May, Marcel Dekker Inc., New York, 1988.

[3] B. Bilyeu, W. Brostow and K. P. Menard, *J. Mater. Ed.*, **21,** 281 (1999).

[4] B. Bilyeu, W. Brostow and K. P. Menard, *J. Mater. Ed.* **22,** 107 (2000).

[5] B. Bilyeu, W. Brostow and K. P. Menard, *Polimery*, **46,** 799 (2001).

[6] B. Wunderlich, *Thermal Analysis*, Academic Press, San Diego, 1990.

[7] F. Szabadvary, *History of Analytical Chemistry*, Pergamon Press, Oxford, 1966.

[8] http://en.wikipedia.org/wiki/Epoxy

[9] H. S. Han, K. L. Tan and E. T. Kang, *J. Appl. Polym. Sci.*, **76,** 296 (2000).

[10] J. P. Pascault, H. Sautereau, J. Verdu and R. J. J Williams, *Thermosetting Polymers*, Marcel Dekker Inc., New York, 2002.

[11] W. Brostow, P. E. Cassidy, J. Macossay, D. Pietkiewicz and S. Venumbaka, *Polym. Int.*, **52,** 1498 (2003).

[12] B. Wunderlich, *Thermal Characterization of Polymeric Materials,* 2nd ed., *e*d. E. Turi, Academic Press, San Diego, 1997.

[13] L. Nuiiez, F. Fraga, L. Fraga, T. Salgado and J. R. Aiion, *Pure Appl. Chem.*, **67,** 1091 (1995).

[14] d' Almeida, G. W. de Menezes, S. N. Monteiro, *Mater. Res.,* **6,** 415 (2003).

[15] http://www.netcomposites.com/education.asp?sequence=11

[16] *Epoxy Book,* System Three Resins Inc.

[17] D. Kotnarowska, *Mater. Sci.*, **14,** 337 (2008)

[18] L. Fogelström, P. Antoni, E. Malmström and A. Hult, *Progr. Org. Coat.*, **55,** 284 (2006).

[19] N. A. Ogurtsov and G. S. Shapoval, *Russ. J. Appl. Chem.*, **79,** 605 (2006).

[20] J. R. Santos, Jr., L. H. C. Mattoso and A. J. Motheo, *Electrochim. Acta,* **43,** 309 (1998).

[21] G. Ahmetli, N. Sen, E. Pehlivan and S. Durak, *Progr. Org. Coat.*, **55,** 262 (2006).

[22] Y. Liu, X. Chen and J. H. Xin, *Nanotechnology*, **17,** 3259 (2006).

[23] A. Kumar, L.D. Stephenson and J.N. Murray, *Progr. Org. Coat.*, **55,** 244 (2006).

[24] I. Skeist, *Epoxy Resins*, Reinhold Publishing, New York, 1958.

[25] J. K. Wise, *J. Paint. Tech.*, **42,** 28 (1970).

[26] D. K. Chattopadhyay, S. S. Panda and K. V. S. N. Raju, *Progr. Org. Coat.*, **54,** 10 (2005).

[27] W. K. Chin, M. D. Shau and W. C. Tsai, *J. Polym. Sci. Chem.,* **33,** 373 (1995).

[28] L. Bazyliak, M. Bratychak and W. Brostow, *Mater. Res. Innovat.,* **3,** 132 (1993).

[29] M. Bratychak and W. Brostow, *Polym. Engng. Sci*., **39,** 1541 (1999).

[30] L. Bazyliak, M. Bratychak and W. Brostow, *Mater. Res. Innovat*., **3**, 218 (2000).

[31] W. Brostow, P. E. Cassidy, H. E. Hagg, M. Jaklewicz and P. E. Montemartini, *Polymer.*, **42,** 7971 (2001).

[32] W. Brostow, B. Bujard, P. E. Cassidy, H. E. Hagg and P. E. Montemartini, *Mater. Res. Innovat*., **6,** 7 (2002).

[33] S. A. Kumar, M. Alagar and V. Mohan, *J. Mater. Engng. Perform.*, **11,** 123 (2002).

[34] K. Saravanan, S. Sathiyanarayanan, S. Muralidharan, S. S. Azim and G. Venkatachari, *Progr. Org. Coat.*, **59,** 160 (2007).

[35] S. Palraj, M. Selvaraj and P. Jayakrishnan, *Progr.Org. Coat.,* **54,** 5 (2005).

[36] P. A. Oyanguren, C. C. Riccardi, R. J. J. Williams and I. Mondragon, *J. Polym. Sci. Phys.*, **36**, 1349 (1998).

[37] E. M. Woo and M. N. Wu, *Polym.*, **37**, 2485 (1996).

[38] A. Aglan, A. Allie, A. Ludwick and L. Koons, *Surf. Coat. Tech.*, **202,** 370 (2007).

[39] S. A. Kumar, T. Balakrishnan, M. Alagar and Z. Denchev, *Progr. Org. Coat.*, **55,** 207 (2006).

[40] S. Ahmad, F. Naqvi, E. Sharmin and K. L. Verma, *Progr. Org. Coat.*, **55,** 268 (2006).

[41] H. J. Yu, L. Wang, Q. Shi, G. H. Jiang, Z. R. Zhao and X. C. Dong, *Progr. Org. Coat.*, **55,** 296 (2006).

[42] T. V. T. Velan and I. M. Bilal, *Bull. Mater. Sci.*, **23,** 425 (2000).

[43] P. M. S. Begum, K. K. Mohammed and R. Joseph, *Int. J. Polym. Mater.,* **57,** 1083 (2008).

[44] M. Muszynska, H. Wycislik and M. Siekierski, *Solid State Ionics*, **147,** 281 (2002).

[45] Y. P. Mamunya, V.V. Davydenko, P. Pissis and E. V. Lebedev, *Europ. Polym. J.*, **38,** 1887 (2002).

[46] S. W. Kim, Y. W. Yoon, S.J. Lee, G. Y. Kim, Y. B. Kim, Y. Y. Chun and K. S. Lee, *J. Magn. Magn. Mater.*, **316,** 472 (2007).

[47] Z. Brito and G. Sanchez, *Compos. Struct.,* **48**, 79 (2000).

[48] K. Gosh and S. N. Maiti, *J. Appl. Polym. Sci.*, **60**, 323 (1996).

[49] W. Brostow, A. Buchman, E. Buchman and O. O. Mejia, *Polym. Eng. Sci.*, **49,** 1977 (2008).

[50] W. Brostow, B. P. Gorman and O. O. Mejia, *Mater. Lett.*, **61,** 1333 (2007).

[51] J. Williams, *Engineering Tribology,* Cambridge University Press, New York, 2005.

[52] B. Bhushan, *Introduction to Tribology,* John Wiley and Sons Inc., New York, 2002.

[53] E. Rabinowicz, *Friction and Wear of Materials,* John Wiley and Sons Inc., 1995.

[54] N. Chan and M. K. Sharma, *Wear*, **264,** 69 (2008).

[55] H. G. Lee, S. S. Kim and D. G. Lee, *Compos. Struct.,* **74,** 136 (2006).

[56] J. M. Thorp, *Trib. Int.,* **15,** 59 (1982).

[57] G. Shi, M. Q. Zhang, M. Z. Rong, B. Wetzel and K. Friedrich, *Wear,* **256,** 1072 (2004).

[58] H. Zhang, Z. Zhang, K. Friedrich and C. Eger, *Acta Mater.,* **54**, 1833 (2006).

[59] M. Q. Zhang, M. Z. Rong, S. L. Yu, B. Wetzel and K. Friedrich, *Wear,* **253,** 1086 (2002).

[60] Z. Zhang, C. Breidt, L. Chang and K. Friedrich, *Trib. Int.,* **37,** 271 (2004).

[61] G. W. Sawyer, K. D. Freudenberg, P. Bhimaraj and L. S. Schadler, *Wear*, **254,** 573 (2003).

[62] Y. M. Xu and B. G. Mellor, *Wear*, **251,** 1522 (2001).

[63] T. Larsen, T. L. Andersen, B. Thorning, A. Horsewell and M. E. Vigild, *Wear,* **262,** 1013 (2007).

[64] W. Brostow, T. H. Grguric, O. O. Mejia, D. Pietkiewicz and V. Rek, *e – Polymers*, **34,** 1 (2008).

[65] V. A. Bely, A. I. Sviridenok, M. I. Petrokovets and V. G. Savkin, *Friction and wear in polymerbased materials,* Pergamon Press, Oxford, 1982.

[66] N. K. Myshkin, M. I. Petrokovets and S. A. Chizhik, *Tribol. Int.*, **31,** 79 (1998).

[67] A. Kovalev, H. Shulga, M. Lemieux, N. Myshkin, V. V. Tsukruk, *J. Mater. Res*., **19,** 716 (2004).

[68] M. I. Petrokovets, *J. Frict. Wear*, **20,** 1 (1999).

[69] H. Hong, *Trib. Int.,* **35**, 725 (2002).

[70] W. Brostow, G. Damarla, J. Howe and D. Pietkiewicz, *e – Polymers,* **25,** 1 (2004).

[71] W. Brostow, H. E. Hagg and M. Narkis, *J. Mater. Res.*, **21,** 2422 (2006).

[72] W. Brostow and H. E. Hagg, *Polym. Eng. Sci.*, **48,** 1982 (2008).

[73] Y. Liu, X. Chen and J. H. Xin, *Nanotechnology,* **17,** 3259 (2006).

[74] http://www.chemcenters.com/images/Epon828.pdf

[75] P. E. Cassidy, T. M. Aminashari and J. M. Farley, *J. Macromol. Sci. Rev. Phys. Chem. C*, **29,** 365 (1989).

[76] G. L. Tullos, P. E. Cassidy, A. K. St. Clair, *Macromolecules,* **24,** 6059 (1991).

[77] http://www.micronmetals.com

[78] J. W. Sinclair, *J. Adhesion*, **38,** 219 (1992).

[79] M. Inoue and K. Suganuma, *Solder. Surf. Mount Tech.,* **18,** 40 (2006).

[80] http://www.speedymetals.com/information/material23.html

[81] W. Brostow, P. E. Cassidy, J. Macossay and D. Pietkiwicz, *Polym. Int*., **52,** 1498 (2003).

[82] http://www.surface-tension.de/

[83] S. Wu, *Polymer Interface and Adhesion*, Marcel Dekker Inc., New York, 1982.

[84] F. J. du Toit, R. D. Sanderson, W. J. Engelbecht and J. B. Wagener, *J. Fluorine Chem.,* **74,** 43 (1995).

[85] M. Arand, R. E. Cohn and R. F. Baddour, *Polymer,* **22,** 361 (1981).

[86] M. Strobel, S. Corn, C. S. Lyons and G. A. Korba, *J. Polym. Sci.: Polym. Chem. ed.,* **23,** 1125 (1985).

[87] *Advances in Chromatography,* ed. P. R. Brown and E. Gruska, Marcel Dekker, New York, 1994.

[88] C. Ramirez, M. Rico, A. Torres, L. Barral, J. Lopez and B. Montero, *Europ. Polym. J*, **44,** 3035 (2008).